



Eidgenössische Technische Hochschule Zürich  
Swiss Federal Institute of Technology Zurich

# Cubical Homology and Applications

Bachelor's Thesis

Nahae Kühn

July 7, 2023

Advisor: Dr. Sara Kališnik Hintz  
Department of Mathematics, ETH Zürich



---

## Abstract

Homology is an invariant in algebraic topology that captures the ‘shape’ of geometric objects, such as the number of loops, cavities, etc. Persistent homology is an adaptation of homology that measures how topology of a nested family of spaces changes with the parameter.

In this thesis, I present an application of cubical persistent homology to satellite images of hurricanes, in particular to quantify the diurnal cycle of hurricanes. Cubical homology as opposed to simplicial homology is built on cubical sets, which are finite unions of cubes with vertices in an integer lattice and can be thought of as a representation of the pixels of the image.



---

# Contents

---

<b>Contents</b>	<b>iii</b>
<b>1 Introduction</b>	<b>1</b>
<b>2 Cubical Homology</b>	<b>5</b>
2.1 Cubical Sets . . . . .	5
2.2 The Algebra of Cubical Sets . . . . .	8
2.2.1 Cubical Chains . . . . .	8
2.2.2 Cubical Chains in Cubical Sets . . . . .	13
2.3 Homology of Cubical Sets . . . . .	16
2.4 The Zeroth Homology Group . . . . .	17
<b>3 Persistent Homology</b>	<b>23</b>
<b>4 Topological Analysis of Tropical Cyclones</b>	<b>35</b>
4.1 Tropical Cyclone Formation & Diurnal Cycles . . . . .	35
4.2 Analysis of Tropical Cyclones using Persistent Homology . .	37
<b>5 Acknowledgement</b>	<b>43</b>
<b>Bibliography</b>	<b>45</b>



## Chapter 1

---

# Introduction

---

Tools to analyze and understand large and complex data sets are becoming more and more important in today's world. One approach to analyzing data is using topological methods. Topology is a branch of mathematics that is concerned with the properties of geometric objects which are unaffected by continuous deformations, such as twisting, stretching or bending. In other words, topology studies the underlying 'shape' of geometric objects.

In algebraic topology, the 'shape' can be captured using homology, which, intuitively speaking, gives the number of loops, cavities, etc. of a space. Consider the example of an annulus, whose difference to a disc is the hole in the middle, or, in other words, the loop in the space. For a topological space, we have infinitely many homology groups. To each homology group, we can assign a betti number. The  $k$ th betti number  $\beta_k$  is the dimension of the  $k$ th homology group and also gives the number of  $(k + 1)$ -dimensional holes:  $\beta_0$  gives the number of connected components, the  $\beta_1$  gives the number of loops,  $\beta_2$  gives the number of cavities, etc. So, the first betti number  $\beta_1$  for the annulus is 1, whereas  $\beta_1$  for the disc is 0. The other betti numbers are all the same for both topological spaces.

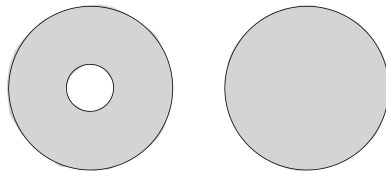


**Figure 1.1:** Left: annulus; right: disc.

Persistent homology is an adaptation of homology that measures how topology of a nested family of spaces changes with the parameter. In the case of images, this family consists of cubical complexes, which are finite unions of

cubes with vertices in an integer lattice. A 0-cube is just a vertex, a 1-cube is an interval, a 2-cube is a square, etc. To convert an image to a cubical complex, we first assign the greyscale value to the corresponding pixel. We can then filter out the squares with an assigned greyscale value over a certain threshold. In Figure 1.2, a greyscale image of a ring-like shape is depicted. We can also consider this image as a cubical set with  $8 \times 8$  squares and all of their edges and vertices, with the greyscale value assigned to each square, like in Figure 1.3. In Figure 1.4, one can see a filtration of this complex consisting of 4 nested cubical complexes corresponding to different thresholds. As the threshold increases, the ring-like structure gets visible. For the maximal threshold, the ring disappears and we only have white squares.

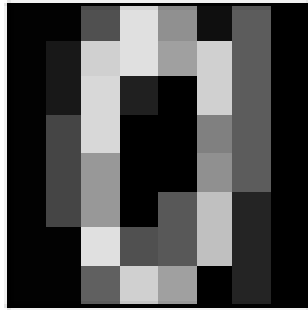


Figure 1.2: A  $8 \times 8$ -greyscale image

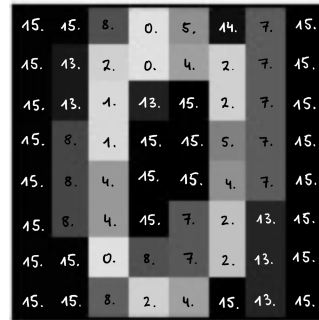


Figure 1.3: The cubical set corresponding with the image with the greyscale values assigned to each square

This framework can be used to analyze satellite images of hurricanes [5], more specifically, to examine 'diurnal' cycles of hurricanes. One of these images can be seen in Figure 1.5.

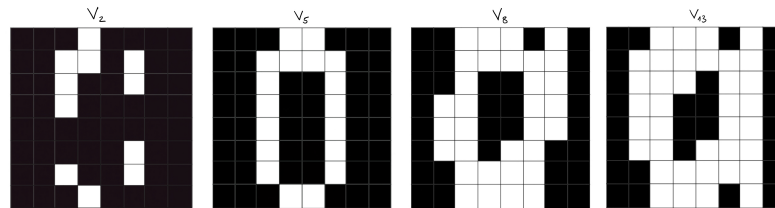


Figure 1.4: filtration of the image on the right with four different thresholds

The diurnal cycle has been described in previous studies [2] and has been observed in infrared satellite imagery as cyclical pulses in the cloud field that propagate radially outward. These pulses form in the core of the hurricane around the time of the local sunset, reach the periphery of the hurricane



---

in the early afternoon of the next day and, because they appear to propagate through a deep layer of the hurricane's environment, they may have implications for the structure and intensity of the hurricane.

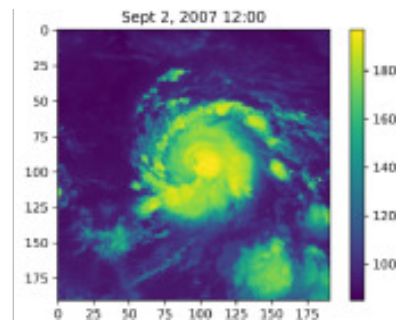


**Figure 1.5:** Original satellite imagery from the hurricane Felix in 2007

This daily cycle is not yet fully understood and lacks quantitative research. In 'Using persistent homology to quantify a diurnal cycle in hurricanes', Tymochko et al. were able to provide a consistent 'method of automatically detecting and quantifying the circular structure in satellite imagery' [5] using topology. In particular, cubical persistent homology was used to analyze infrared images of the hurricanes Felix in 2007 and Ivan in 2004, which were taken hourly. It was established that the frequency is approximately 1 cycle per day.



## Chapter 2

---

# Cubical Homology

---

In this chapter, we introduce cubical homology and cubical sets, which are sets based on vertices in an integer lattice. We will closely follow the textbook ‘Computational Homology’ by Tomasz Kazynski, et al. ([3], p.39-63).

## 2.1 Cubical Sets

**Definition 2.1** *An elementary interval is a closed interval  $I \subset \mathbb{R}$  of the form*

$$I = [l, l + 1] \text{ or } I = [l]$$

*for some  $l \in \mathbb{Z}$ . To simplify the notation, we write  $[l] = [l, l]$  for an interval that contains only one point. Elementary intervals that consist of a single point are degenerate, while those of length 1 are nondegenerate.*

**Example 2.2**  $[14]$  and  $[2, 3]$  are elementary intervals.  $[\frac{2}{3}]$  is not an elementary interval because  $\frac{2}{3} \notin \mathbb{Z}$ .  $[7, 9]$  is not an elementary interval because the length of the interval is greater than 1.

**Definition 2.3** *An elementary cube  $Q$  is a finite product of elementary intervals, that is,*

$$Q = I_1 \times I_2 \times \cdots \times I_d \in \mathbb{R}^d,$$

*where each  $I_i$  is an elementary interval. The set of all elementary cubes in  $\mathbb{R}^d$  is denoted by  $\mathcal{K}^d$ . The set of all elementary cubes is denoted by  $\mathcal{K}$ , namely*

$$\mathcal{K} := \bigcup_{d=1}^{\infty} \mathcal{K}^d$$

**Example 2.4** *Figure 2.1 depicts some examples of elementary cubes. The cubes  $[6] \times [2, 3]$  and  $[7, 8] \times [2]$  have one degenerate and one non-degenerate component, whereas  $[7, 8] \times [2, 3]$  has two non-degenerate components.*

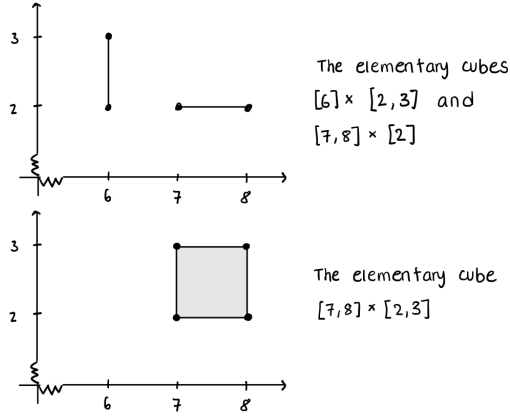


Figure 2.1: Examples of elementary cubes in  $\mathbb{R}^2$ .

**Definition 2.5** Let  $Q = I_1 \times I_2 \times \cdots \times I_d \in \mathbb{R}^d$  be an elementary cube. The embedding number of  $Q$  is denoted by  $\text{emb } Q$  and is defined to be  $d$  since  $Q \subset \mathbb{R}^d$ . The interval  $I_i$  is referred to as the  $i$ -th component of  $Q$  and is written as  $I_i(Q)$ . The dimension of  $Q$  is defined to be the number of nondegenerate components on  $Q$  and is denoted by  $\text{dim } Q$ .

Observe that if  $\text{emb } Q = d$ , then  $Q \in \mathcal{K}^d$ . We also let

$$\mathcal{K}_k := \{Q \in \mathcal{K} \mid \text{dim } Q = k\}$$

and

$$\mathcal{K}_k^d := \mathcal{K}_k \cap \mathcal{K}^d.$$

**Example 2.6** The embedding number of  $Q_1 = [2, 3] \times [7, 8] \times [1]$  is  $\text{emb } Q_1 = 3$ . The dimension of  $Q_1$  is  $\text{dim } Q_1 = 2$ , because  $Q_1$  has 2 nondegenerate elementary intervals. For the elementary cube in Figure 2.1, we get the following embedding numbers and dimensions:

$$\begin{aligned} \text{emb } [6] \times [2, 3] &= \text{emb } [7, 8] \times [2] = \text{emb } [7, 8] \times [2, 3] = 2 \\ \text{dim } [6] \times [2, 3] &= \text{dim } [7, 8] \times [2] = 1 \\ \text{dim } [7, 8] \times [2, 3] &= 2. \end{aligned}$$

**Proposition 2.7** Let  $Q \in \mathcal{K}_k^d$  and  $P \in \mathcal{K}_{k'}^{d'}$ . Then

$$Q \times P \in \mathcal{K}_{k+k'}^{d+d'}.$$

**Proof** Because  $Q \in \mathcal{K}^d$ , it can be written as the product of  $d$  elementary intervals:

$$Q = I_1 \times I_2 \times \cdots \times I_d.$$

Similarly,

$$P = J_1 \times J_2 \times \dots \times J_{d'},$$

where each  $J_i$  is an elementary interval. Hence,

$$Q \times P = I_1 \times I_2 \times \dots \times I_d \times J_1 \times J_2 \times \dots \times J_{d'},$$

which is a product of  $d + d'$  elementary intervals. The dimension, or rather the number of nondegenerate components of  $Q$ , is  $k$  and  $k'$  is the dimension of  $P$ . Then the product  $Q \times P$  has  $(k + k')$  nondegenerate components, thus  $\dim(Q \times P) = \dim Q + \dim P$ .  $\square$

**Definition 2.8** Let  $Q, P \in \mathcal{K}$ . If  $Q \subset P$ , then  $Q$  is a face of  $P$ . This is denoted by  $Q \preceq P$ . If  $Q \preceq P$  and  $Q \neq P$ , then  $Q$  is a proper face of  $P$ , which is written as  $Q \prec P$ .  $Q$  is a primary face of  $P$  if  $Q$  is a face of  $P$  and  $\dim Q = \dim P - 1$ .

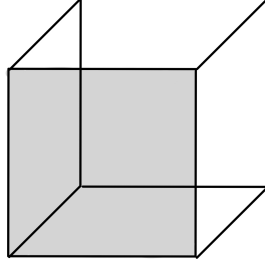


**Figure 2.2:** The elementary cube  $Q = [0, 1] \times [0, 1] \times [0, 1]$

**Example 2.9** A primary face of  $Q = [0, 1] \times [0, 1] \times [0, 1]$  would be the two-dimensional cube  $[0, 1] \times [0] \times [0, 1]$ , which is also marked grey in figure 2.2. Any vertex of  $Q$  is also a face of  $Q$ .

**Definition 2.10** A set  $X \subset \mathbb{R}^d$  is cubical if  $X$  can be written as a finite union of elementary cubes. If  $X \subset \mathbb{R}^d$  is a cubical set, then we adopt the following notation:

$$\mathcal{K}(X) := \{Q \in \mathcal{K} \mid Q \subset X\}$$

and

$$\mathcal{K}_k(X) := \{Q \in \mathcal{K}(X) \mid \dim Q = k\}.$$

Observe that if  $Q \subset X$  and  $Q \in \mathcal{K}$ , then  $\dim Q = d$ , since  $X \subset \mathbb{R}^d$ . This in turn implies that  $Q \in \mathcal{K}^d$ , so to use the notation  $\mathcal{K}^d(X)$  is somewhat redundant, but it serves to remind us that  $X \subset \mathbb{R}^d$ . Therefore, when it is convenient, we will write  $\mathcal{K}^d(X)$  and also  $\mathcal{K}_k^d(X) := \mathcal{K}^d(X) \cap \mathcal{K}_k(X)$ . In analogy with graphs, the elements of  $\mathcal{K}_0(X)$  are the vertices and the elements of  $\mathcal{K}_1(X)$  are the edges of  $X$ . More generally, the elements of  $\mathcal{K}_k(X)$  are the  $k$ -cubes of  $X$ .

**Example 2.11** Let  $X = [0, 1] \times [0, 1] \times [0, 1] \subset \mathbb{R}^3$ .  $X$  is an elementary cube and hence a cubical set. The  $k$ -cubes for  $k = 0, 1, 2$  are

- $\mathcal{K}_2(X) = \{[0] \times [0, 1] \times [0, 1], [1] \times [0, 1] \times [0, 1], [0, 1] \times [0] \times [0, 1], [0, 1] \times [1] \times [0, 1], [0, 1] \times [0, 1] \times [0], [0, 1] \times [0, 1] \times [0]\}$
- $\mathcal{K}_1(X) = \{[0] \times [0] \times [0, 1], [1] \times [0] \times [0, 1], [0] \times [1] \times [0, 1], [1] \times [1] \times [0, 1], [0] \times [0, 1] \times [0], [1] \times [0, 1] \times [0], [0] \times [0, 1] \times [1], [1] \times [0, 1] \times [1], [0, 1] \times [0] \times [0], [0, 1] \times [0] \times [1], [0, 1] \times [1] \times [0], [0, 1] \times [1] \times [1]\}$
- $\mathcal{K}_0(X) = \{[0] \times [0] \times [0], [0] \times [0] \times [1], [0] \times [1] \times [0], [1] \times [0] \times [0], [0] \times [1] \times [1], [1] \times [0] \times [1], [1] \times [1] \times [0], [1] \times [1] \times [1]\}$ .

**Proposition 2.12** *If  $X \subset \mathbb{R}^d$  is cubical, then  $X$  is closed and bounded.*

**Proof** By definition a cubical set is a finite union of elementary cubes. Elementary cubes are a finite product of elementary intervals, which are closed. One can show by induction on  $d$  that the product of elementary intervals  $I_1, \dots, I_d \subset \mathbb{R}$  is a closed subset of  $\mathbb{R}^d$ . Moreover, the finite union of closed sets is closed.

To show that  $X$  is bounded, it is sufficient to prove that for some  $R > 0$ ,

$$X \subset B_0(0, R), \quad (2.1)$$

where  $B_0(0, R)$  denotes the ball around the origin in the supremum norm. Let  $Q \in \mathcal{K}(X)$ . Then  $Q = I_1 \times \dots \times I_d$ , where  $I_i = [l_i]$  or  $I_i = [l_i, l_i + 1]$ . Let

$$\rho(Q) = \max_{\{i=1, \dots, d\}} \{|l_i| + 1\}$$

Taking  $R := \max_{\{Q \in \mathcal{K}(X)\}} \rho(Q)$ , one can verify 2.1. □

## 2.2 The Algebra of Cubical Sets

Now that we have build the actual geometric cubical sets, we want to give the formal definitions needed to define cubical homology. So, we move on to viewing elementary cubes as algebraic objects and to do mathematical operations with them.

### 2.2.1 Cubical Chains

**Definition 2.13** *With each elementary  $k$ -cube  $Q \in \mathcal{K}_k^d$ , we associate an algebraic object  $\hat{Q}$  called an elementary  $k$ -chain of  $\mathbb{R}^d$ . The set of all elementary  $k$ -chains of  $\mathbb{R}^d$  is denoted by*

$$\hat{\mathcal{K}}_k^d := \{\hat{Q} \mid Q \in \mathcal{K}_k^d\}.$$

*Given any finite collection  $\{\hat{Q}_1, \dots, \hat{Q}_m\} \subset \hat{\mathcal{K}}_k^d$  of  $k$ -dimensional elementary chains, we are allowed to consider sums of the form*

$$c = \alpha_1 \hat{Q}_1 + \alpha_2 \hat{Q}_2 + \dots + \alpha_m \hat{Q}_m,$$

where  $\alpha_i$  are arbitrary integers. If all the  $\alpha_i = 0$ , then we let  $c = 0$ . These can be thought of as our  $k$ -chains, the set of which is denoted by  $C_k^d$ . The addition of  $k$ -chains is naturally defines by

$$\sum \alpha_i \hat{Q}_i + \sum \beta_i \hat{Q}_i := \sum (\alpha_i + \beta_i) \hat{Q}_i$$

Observe that given an arbitrary  $k$ -chain  $c = \sum_{i=0}^m \alpha_i \hat{Q}_i$ , there is an inverse element  $-c = \sum_{i=0}^m (-\alpha_i) \hat{Q}_i$  with the property that  $c + (-c) = 0$ . Therefore,  $C_k^d$  is an abelian group and, in fact, it is a free abelian group with basis  $\hat{\mathcal{K}}_k^d$ .

Another prescription for using a set to generate a free abelian group involves viewing the chains as functions from  $\mathcal{K}_k^d$  to  $\mathbb{Z}$ . In particular, for each  $Q \in \mathcal{K}_k^d$ , define  $\hat{Q} : \mathcal{K}_k^d \rightarrow \mathbb{Z}$  by

$$\hat{Q}(P) := \begin{cases} 1 & \text{if } P = Q \\ 0 & \text{otherwise.} \end{cases}$$

**Definition 2.14** The group  $C_k^d$  of  $k$ -dimensional chains of  $\mathbb{R}^d$  is the free abelian group generated by the elementary chains of  $\mathcal{K}_k^d$ . Thus the elements of  $C_k^d$  are functions  $c : \mathcal{K}_k^d \rightarrow \mathbb{Z}$  such that  $c(Q) = 0$  for all but a finite number of  $Q \in \mathcal{K}_k^d$ . In particular,  $\hat{\mathcal{K}}_k^d$  is a basis for  $C_k^d$  (in other notation:  $C_k^d = \mathbb{Z}(\hat{\mathcal{K}}_k^d)$ ). If  $c \in C_k^d$ , then  $\dim c := k$ .

Obviously, since the elementary cubes are contained in  $\mathbb{R}^d$ , for  $k \leq 0$  and  $k \geq d$ , the set  $\mathcal{K}_k = \emptyset$  and the corresponding group of  $k$ -chains is  $C_k^d = 0$ .

**Proposition 2.15** The map  $\varphi : \mathcal{K}_k^d \rightarrow \hat{\mathcal{K}}_k^d$  given by  $\varphi(Q) = \hat{Q}$  is a bijection.

**Proof** Because  $\hat{\mathcal{K}}_k^d$  is defined to be the image of  $\varphi$ , it is obvious that  $\varphi$  is surjective. To prove injectivity, assume that  $P, Q \in \mathcal{K}_k^d$  and  $\hat{P} = \hat{Q}$ . This implies that  $1 = \hat{P}(P) = \hat{Q}(P)$  and hence that  $P = Q$ .  $\square$

**Definition 2.16** Let  $c \in C_k^d$ . The support of the chain  $c$  is the cubical set

$$|c| := \bigcup \{Q \in \mathcal{K}_k^d \mid c(Q) \neq 0\}.$$

**Example 2.17** As an example, take again  $Q = [0, 1] \times [0, 1] \times [0, 1]$  and the chain

$$c = 2[0] \times [0, 1] \times [0, 1] - [0, 1] \times [0, 1] \times [0] + [1] \times [0, 1] \times [0, 1] + [0, 1] \times [0, 1] \times [1].$$

Then the support of  $c$  is the set

$$|c| = \{[0] \times [0, 1] \times [0, 1], [0, 1] \times [0, 1] \times [0], [1] \times [0, 1] \times [0, 1], [0, 1] \times [0, 1] \times [1]\},$$

which is also marked grey in figure 2.3.

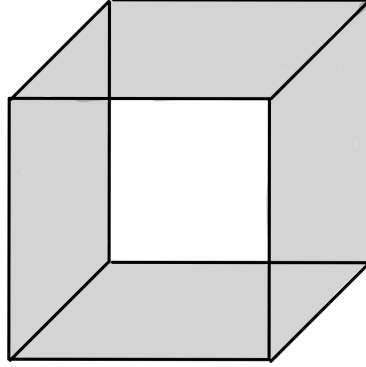


**Figure 2.3:** The elementary cube  $Q = [0, 1] \times [0, 1] \times [0, 1]$

The support has several convenient geometric features.

**Proposition 2.18** *The support satisfies the following properties:*

(i)  $|c| = \emptyset$  iff  $c = 0$ .

(ii) Let  $\alpha \in \mathbb{Z}$  and  $c \in C_k^d$ . Then

$$|\alpha c| = \begin{cases} \emptyset & \text{if } \alpha = 0 \\ |c| & \text{if } \alpha \neq 0. \end{cases}$$

(iii) If  $Q \in \mathcal{K}$ , then  $|\hat{Q}| = Q$ .

(iv) If  $c_1, c_2 \in C_k^d$ , then  $|c_1 + c_2| \subset |c_1| \cup |c_2|$ .

**Proof** (i) In the case of the 0-chain for every  $Q \in \mathcal{K}_k^d$  the value  $0(Q) = 0$ . Therefore,  $|c| = \emptyset$ . On the other hand, if  $|c| = \emptyset$ , then there is no  $Q$  such that  $c(Q) \neq 0$ . Therefore,  $c = 0$ .

(ii) This follows directly from the definition of the support and (i).

(iii) This follows from the definition of elementary chains.

(iv) Let  $x \in |c_1 + c_2|$ . Then  $x \in Q$  for some  $Q \in \mathcal{K}_k^d$  such that

$$(c_1 + c_2)(Q) = c_1(Q) + c_2(Q) \neq 0.$$

It follows that either  $c_1(Q) \neq 0$  or  $c_2(Q) \neq 0$ , hence  $x \in |c_1|$  or  $x \in |c_2|$ .

□

**Definition 2.19** Consider  $c_1, c_2 \in C_k^d$ , where  $c_1 = \sum_{i=1}^m \alpha_i \hat{Q}_i$  and  $c_2 = \sum_{i=1}^m \beta_i \hat{Q}_i$ . The scalar product of the chains  $c_1$  and  $c_2$  is defined as

$$\langle c_1, c_2 \rangle := \sum_{i=1}^m \alpha_i \beta_i$$



**Proposition 2.20** *The scalar product defines a mapping*

$$\langle \cdot, \cdot \rangle: \mathbb{C}_k^d \times \mathbb{C}_k^d \rightarrow \mathbb{Z}$$

$$(c_1, c_2) \mapsto \langle c_1, c_2 \rangle$$

**Proof** We need to show that the map is bilinear, symmetric and positive definite. Additivity, symmetry and positive definiteness follow directly from the definition. What is left to show is  $\langle \alpha c_1 + \beta c_2, c_3 \rangle = \alpha \langle c_1, c_3 \rangle + \beta \langle c_2, c_3 \rangle$  and  $\langle c_1, \alpha c_2 + \beta c_3 \rangle = \alpha \langle c_1, c_2 \rangle + \beta \langle c_1, c_3 \rangle$ . For  $j = 1, 2, 3$ , let

$$c_j = \sum_{i=1}^m \gamma_{j,i} \hat{Q}_i$$

Then

$$\begin{aligned} \langle \alpha c_1 + \beta c_2, c_3 \rangle &= \left\langle \alpha \sum_{i=1}^m \gamma_{1,i} \hat{Q}_i + \beta \sum_{i=1}^m \gamma_{2,i} \hat{Q}_i, \sum_{i=1}^m \gamma_{3,i} \hat{Q}_i \right\rangle \\ &= \left\langle \sum_{i=1}^m (\alpha \gamma_{1,i} + \beta \gamma_{2,i}) \hat{Q}_i, \sum_{i=1}^m \gamma_{3,i} \hat{Q}_i \right\rangle \\ &= \sum_{i=1}^m (\alpha \gamma_{1,i} + \beta \gamma_{2,i}) \gamma_{3,i} \\ &= \alpha \sum_{i=1}^m \gamma_{1,i} \gamma_{3,i} + \beta \sum_{i=1}^m \gamma_{2,i} \gamma_{3,i} \\ &= \alpha \left\langle \sum_{i=1}^m \gamma_{1,i} \hat{Q}_i, \sum_{i=1}^m \gamma_{3,i} \hat{Q}_i \right\rangle + \beta \left\langle \sum_{i=1}^m \gamma_{2,i} \hat{Q}_i, \sum_{i=1}^m \gamma_{3,i} \hat{Q}_i \right\rangle \\ &= \alpha \langle c_1, c_3 \rangle + \beta \langle c_2, c_3 \rangle. \end{aligned}$$

The proof of the other equality  $\langle c_1, \alpha c_2 + \beta c_3 \rangle = \alpha \langle c_1, c_2 \rangle + \beta \langle c_1, c_3 \rangle$  is analogous.  $\square$

**Definition 2.21** *Given two elementary cubes  $P \in \mathcal{H}_k^d$  and  $Q \in \mathcal{H}_{k'}^{d'}$  set*

$$\hat{P} \diamond \hat{Q} := \widehat{P \times Q}.$$

*This definition extends to arbitrary chains  $c_1 \in \mathbb{C}_k^d$  and  $c_2 \in \mathbb{C}_{k'}^{d'}$  by*

$$c_1 \diamond c_2 := \sum_{P \in \mathcal{H}_k, Q \in \mathcal{H}_{k'}} \langle c_1, \hat{P} \rangle \langle c_2, \hat{Q} \rangle \widehat{P \times Q}.$$

*The chain  $c_1 \diamond c_2 \in \mathbb{C}_{k+k'}^{d+d'}$  is called the cubical product of  $c_1$  and  $c_2$ .*

**Example 2.22** *The cubical product is not commutative, e.g. take the elementary cubes  $P_1 = [0, 1]$ ,  $P_2 = [1, 2]$  and  $Q_1 = [0, 1] \times [1]$ ,  $Q_2 = [1] \times [0, 1]$  and the chains  $c_1 = \hat{P}_1 + \hat{P}_2$ ,  $c_2 = \hat{Q}_1 + \hat{Q}_2$ . Then*

$$\begin{aligned} c_1 \diamond c_2 &= \langle c_1, \hat{P}_1 \rangle \langle c_2, \hat{Q}_1 \rangle \widehat{P_1 \times Q_1} + \dots + \langle c_1, \hat{P}_2 \rangle \langle c_2, \hat{Q}_2 \rangle \widehat{P_2 \times Q_2} \\ &= \widehat{P_1 \times Q_1} + \widehat{P_1 \times Q_2} + \widehat{P_2 \times Q_1} + \widehat{P_2 \times Q_2} \end{aligned}$$

and

$$c_1 \diamond c_2 = \widehat{Q_1 \times P_1} + \widehat{Q_1 \times P_2} + \widehat{Q_2 \times P_1} + \widehat{Q_2 \times P_2}.$$

So we have  $c_1 \diamond c_2 \neq c_2 \diamond c_1$ .

**Proposition 2.23** *Let  $c_1, c_2, c_3$  be any chains.*

- (i)  $c_1 \diamond 0 = 0 \diamond c_1 = 0$ .
- (ii)  $c_1 \diamond (c_2 + c_3) = c_1 \diamond c_2 + c_1 \diamond c_3$ , provided  $c_2, c_3 \in C_k^d$ .
- (iii)  $(c_1 \diamond c_2) \diamond c_3 = c_1 \diamond (c_2 \diamond c_3)$ .
- (iv) If  $c_1 \diamond c_2 = 0$ , then  $c_1 = 0$  or  $c_2 = 0$ .
- (v)  $|c_1 \diamond c_2| = |c_1| \times |c_2|$ .

**Proof** (i) and (ii) follow immediately from the definition.

(iii) The proof is straightforward.

(iv) Assume that  $c_1 = \sum_{i=1}^m \alpha_i \hat{P}_i$  and  $c_2 = \sum_{j=1}^n \beta_j \hat{Q}_j$ . Then

$$\sum_{i=1}^m \sum_{j=1}^n \alpha_i \beta_j \hat{P}_i \diamond \hat{Q}_j = 0,$$

that is,  $\alpha_i \beta_j = 0$  for any  $i = 1, 2, \dots, m$  and  $j = 1, 2, \dots, n$ . It follows that

$$0 = \sum_{i=1}^m \sum_{j=1}^n (\alpha_i \beta_j)^2 = \left( \sum_{i=1}^m \alpha_i^2 \right) \left( \sum_{j=1}^n \beta_j^2 \right),$$

hence,  $\sum_{i=1}^m \alpha_i^2 = 0$  or  $\sum_{j=1}^n \beta_j^2 = 0$ . Consequently,  $c_1 = 0$  or  $c_2 = 0$ .

(v) Let  $c_1 \in C_k^d$  and  $c_2 \in C_{k'}^d$ . We use the definitions of the support and of the cubical product  $c_1 \diamond c_2$ :

$$\begin{aligned} |c_1 \diamond c_2| &= \bigcup \{P \times Q \in \mathcal{K}_{k+k'} \mid c_1 \diamond c_2(P \times Q) \neq 0\} \\ &= \bigcup \{P \times Q \in \mathcal{K}_{k+k'} \mid \sum_{P \in \mathcal{K}_k, Q \in \mathcal{K}_{k'}} \langle c_1, \hat{P} \rangle \langle c_2, \hat{Q} \rangle P \times Q \neq 0\} \\ &= \bigcup \{P \times Q \in \mathcal{K}_{k+k'} \mid c_1(P) \neq 0 \wedge c_2(Q) \neq 0\} \\ &= \bigcup \{P \in \mathcal{K}_k \mid c_1(P) \neq 0\} \times \bigcup \{Q \in \mathcal{K}_{k'} \mid c_2(Q) \neq 0\} \\ &= |c_1| \times |c_2|. \quad \square \end{aligned}$$

**Proposition 2.24** *Let  $\hat{Q}$  be an elementary cubical chain of  $\mathbb{R}^d$  with  $d > 1$ . Then there exist unique elementary cubical chains  $\hat{I}$  and  $\hat{P}$  with the embedding numbers  $\text{emb } I = 1$  and  $\text{emb } P = d - 1$  such that*

$$\hat{Q} = \hat{I} \diamond \hat{P}.$$

**Proof** Since  $\hat{Q}$  is an elementary cubical chain,  $Q$  is an elementary cube, namely  $Q = I_1 \times \dots \times I_d$ . Set  $I := I_1$  and  $P := I_2 \times \dots \times I_d$ . Then,  $\hat{Q} = \hat{I} \diamond \hat{P}$ . We still need to prove that this is the unique decomposition. If  $\hat{Q} = \hat{J} \diamond \hat{P}'$  for some  $J \in \mathcal{K}^1$  and  $P' \in \mathcal{K}^{d-1}$ , then  $\widehat{I_1 \times P} = \widehat{J \times P'}$  and from Proposition 2.15 we obtain  $I_1 \times P = J \times P'$ . Since  $I_1, J \subset \mathbb{R}$ , it follows that  $I_1 = J$  and  $P = P'$ .  $\square$

### 2.2.2 Cubical Chains in Cubical Sets

Now, since we have discussed cubical chains in general, we can move on to study them in the context of cubical sets.

**Definition 2.25** Let  $X \subset \mathbb{R}^d$  be a cubical set. Let  $\hat{\mathcal{K}}_k(X) := \{\hat{Q} \mid Q \in \mathcal{K}_k(X)\}$ .  $C_k(X)$  is the cubical subgroup of  $C_k^d$  generated by the elements of  $\hat{\mathcal{K}}_k(X)$  and is referred to as the set of  $k$ -chains of  $X$ . In other words,

$$C_k(X) = \{c \in C_k^d \mid |c| \subset X\}. \quad (2.2)$$

Since we know that  $X \subset \mathbb{R}^d$ , it is not necessary to write a superscript  $d$  in  $\hat{\mathcal{K}}_k(X)$  and  $C_k(X)$ .

$\hat{\mathcal{K}}_k(X)$  is a basis of  $C_k(X)$ . Moreover, since for any cubical set  $X$  the family  $\mathcal{K}_k(X)$  is finite,  $C_k(X)$  is a finite-dimensional free abelian group. Finally given any  $c \in C_k(X)$ , we have the decomposition

$$c = \sum_{Q_i \in \mathcal{K}_k(X)} \alpha_i \hat{Q}_i,$$

where  $\alpha_i := c(Q_i)$ . An equivalent formula using the scalar product would be

$$c = \sum_{Q \in \mathcal{K}_k(X)} \langle c, \hat{Q} \rangle \hat{Q}.$$

**Definition 2.26** Given  $k \in \mathbb{Z}$ , the cubical boundary operator or cubical boundary map

$$\partial : C_k^d \rightarrow C_{k-1}^d$$

is a homomorphism of free abelian groups, which is defined for an elementary chain  $\hat{Q} \in \hat{\mathcal{K}}_k^d$  by induction on the embedding number  $d$  as follows:

Consider first the case  $d = 1$ . Then  $Q$  is an elementary interval and hence  $Q = [l] \in \mathcal{K}_0^1$  or  $Q = [l, l+1] \in \mathcal{K}_1^1$  for some  $l \in \mathbb{Z}$ . Define

$$\partial_k \hat{Q} := \begin{cases} 0 & \text{if } Q = [l], \\ \widehat{[l+1]} - \widehat{[l]} & \text{if } Q = [l, l+1]. \end{cases}$$

Now assume that  $d > 1$ . Let  $I = I_1(Q)$  and  $P = I_2(Q) \times \dots \times I_d(Q)$ . Then by Proposition 2.24,  $\hat{Q} = \hat{I} \times \hat{P}$ . Define

$$\partial_k \hat{Q} := \partial_{k_1} \hat{I} \diamond \hat{P} + (-1)^{\dim I} \hat{I} \diamond \partial_{k_2} \hat{P},$$

where  $k_1 = \dim I$  and  $k_2 = \dim P$ .

Finally, we extend the definition to all chains by linearity: If

$$c = \alpha_1 \hat{Q}_1 + \alpha_2 \hat{Q}_2 + \dots + \alpha_m \hat{Q}_m,$$

then

$$\partial_k c := \alpha_1 \partial_k \hat{Q}_1 + \alpha_2 \partial_k \hat{Q}_2 + \dots + \alpha_m \partial_k \hat{Q}_m.$$

**Example 2.27** The cubical boundary of the square  $[0, 1] \times [0, 1]$  is

$$\begin{aligned} \partial_2([0, 1] \times [0, 1]) &= \partial_1 \widehat{[0, 1]} \diamond \widehat{[0, 1]} + (-1)^{\dim [0, 1]} \widehat{[0, 1]} \diamond \partial_1 \widehat{[0, 1]} \\ &= ([\hat{1}] - [\hat{0}]) \diamond \widehat{[0, 1]} - \widehat{[0, 1]} \diamond ([\hat{1}] - [\hat{0}]) \\ &= [1] \times \widehat{[0, 1]} - [0] \times \widehat{[0, 1]} - \widehat{[0, 1]} \times [1] + \widehat{[0, 1]} \times [0]. \end{aligned}$$

Usually, we omit the subscript of the boundary map  $\partial_k$ , because  $k$  is usually clear from the context.

**Proposition 2.28**  $\partial \circ \partial = 0$ .

**Proof** Because  $\partial$  is a linear operator it suffices to show this property for elementary cubical chains. We proceed by induction on the embedding number.

Let  $Q$  be an elementary interval. If  $Q = [l]$ , then by definition  $\partial \hat{Q} = 0$ , so  $\partial(\partial \hat{Q}) = 0$ . If  $Q = [l, l + 1]$ , then

$$\begin{aligned} \partial(\partial \hat{Q}) &= \partial(\partial \widehat{[l, l + 1]}) \\ &= \partial(\widehat{[l, l + 1]} - [\hat{l}]) \\ &= \partial \widehat{[l, l + 1]} - \partial [\hat{l}] \\ &= 0 - 0. \end{aligned}$$

Now assume that  $Q \in \mathcal{K}^d$  for  $d > 1$ . Then  $Q = I \times P$ , where  $I = I_1(Q)$  and  $P = I_2(Q) \times \dots \times I_d(Q)$ . So, by Proposition 2.24,

$$\begin{aligned} \partial(\partial \hat{Q}) &= \partial(\partial \widehat{I \times P}) \\ &= \partial(\partial(\hat{I} \times \hat{P})) \\ &= \partial(\partial \hat{I} \diamond \hat{P} + (-1)^{\dim \hat{I}} \hat{I} \diamond \partial \hat{P}) \\ &= \partial(\partial \hat{I} \diamond \hat{P}) + (-1)^{\dim \hat{I}} \partial(\hat{I} \diamond \partial \hat{P}) \\ &= \partial \partial \hat{I} \diamond \hat{P} + (-1)^{\dim \partial \hat{I}} \partial \hat{I} \diamond \partial \hat{P} + (-1)^{\dim \hat{I}} \partial(\hat{I} \diamond \partial \hat{P}) \\ &= (-1)^{\dim \partial \hat{I}} \partial \hat{I} \diamond \partial \hat{P} + (-1)^{\dim \hat{I}} (\partial \hat{I} \diamond \partial \hat{P} + (-1)^{\dim \hat{I}} \hat{I} \diamond \partial \partial \hat{P}) \\ &= (-1)^{\dim \partial \hat{I}} \partial \hat{I} \diamond \partial \hat{P} + (-1)^{\dim \hat{I}} \partial \hat{I} \diamond \partial \hat{P}. \end{aligned}$$

The last step uses the induction hypothesis that the proposition is true is the embedding number is less than  $d$ .

Observe that if  $\dim \hat{I} = 0$ , then  $\partial \hat{I} = 0$ , in which case we have that each term in the sum is 0 and hence  $\partial \partial \hat{Q} = 0$ . On the other hand, if  $\dim \hat{I} = 1$ , then  $\dim \partial \hat{I} = 0$  and hence the two terms cancel each other, giving the desired result.  $\square$

**Proposition 2.29** For any chain  $c \in C_k^d$ ,

$$|\partial c| \subset |c|.$$

Moreover,  $|\partial c|$  is contained in the union of  $(k-1)$ -dimensional faces of  $|c|$ .

**Proof** First consider the case when  $c = \hat{Q}$ , where  $Q$  is given by the product  $Q = I_1(Q) \times I_2(Q) \times \dots \times I_k(Q) \in \mathcal{K}_k$ . The boundary of  $\hat{Q}$  is given by

$$\partial \hat{Q} = \partial \hat{I} \diamond \hat{P} + (-1)^{\dim I} \hat{I} \diamond \partial \hat{P}.$$

One can see that the support of each nonzero term of the sum is the union of two parallel  $(k-1)$ -dimensional faces of  $Q$ . Thus,

$$|\partial \hat{Q}| \subset \bigcup \mathcal{K}_{k-1}(Q) \subset Q = |\hat{Q}|.$$

If  $c$  is arbitrary, then  $c = \sum_i \alpha_i \hat{Q}_i$  for some  $\alpha_i \neq 0$  and

$$|\partial c| = \left| \sum_i \alpha_i \partial \hat{Q}_i \right| \subset \bigcup_i |\partial \hat{Q}_i| \subset \bigcup_i |\hat{Q}_i| = |c|. \quad \square$$

**Proposition 2.30** Let  $X \in \mathbb{R}^d$  be a cubical set. Then  $\partial_k(C_k(X)) \subset C_{k-1}(X)$ .

**Proof** Let  $c \in C_k(X)$ . Then by equation 2.29,  $|c| \subset X$ , and by Proposition 2.28,  $|\partial_k(c)| \subset |c| \subset X$ . Therefore,  $\partial_k(c) \in C_{k-1}(X)$ .  $\square$

From proposition 2.30, it follows directly that the restriction of the boundary operator  $\partial$  to chains in  $X$ , which we write as  $\partial_k^X : C_k(X) \rightarrow C_{k-1}(X)$ , is well defined.

**Definition 2.31** The cubical chain complex for the cubical set  $X \in \mathbb{R}^d$  is

$$\mathcal{C}(X) := \{C_k(X), \partial_k^X\}_{k \in \mathbb{Z}},$$

Where  $C_k(X)$  are the groups of cubical  $k$ -chains generated by  $\mathcal{K}_k(X)$  and  $\partial_k^X$  is as defined above.

### 2.3 Homology of Cubical Sets

We can now give the most important definition of this chapter, which is the definition of homology groups.

**Definition 2.32** Let  $X \subset \mathbb{R}^d$  be a cubical set and  $\mathcal{C}(X)$  the corresponding chain complex. A  $k$ -chain  $z \in C_k(X)$  is called a cycle in  $X$  if  $\partial z = 0$ . Because the kernel of a linear map is a subgroup of the domain, the set of all  $k$ -cycles in  $X$   $\ker \partial_k^X$ , which is denoted by  $Z_k(X)$ , forms a subgroup of  $C_k(X)$ .

A  $k$ -chain  $z \in C_k(X)$  is a boundary in  $X$  if there exists  $c \in C_{k+1}(X)$ , such that  $\partial c = z$ . Thus the set of boundary elements in  $C_k(X)$ , which is denoted by  $B_k(X)$ , consists of the image of  $\partial_{k+1}^X$ . Since  $\partial_{k+1}^X$  is a homomorphism,  $B_k(X)$  is a subgroup of  $C_k(X)$ .

By proposition 2.28,  $\partial c = z$  implies  $\partial z = \partial^2 c = 0$ . Hence every boundary is a cycle and  $B_k(X)$  is a subgroup of  $Z_k(X)$ . We are interested in cycles that are not boundaries and thus want to treat cycles that are boundaries as trivial. Thus we define the  $k$ -th cubical homology group of  $X$  to be the quotient group

$$H_k(X) := \ker \partial_k^X / \text{im } \partial_{k+1}^X = Z_k(X) / B_k(X).$$

**Example 2.33** We want to compute the homology groups of the set

$$X = [0] \times [0, 1] \cup [0, 1] \times [0] \cup [1] \times [0, 1] \cup [0, 1] \times [1].$$

The elementary cubes of  $X$  are

$$\begin{aligned} \mathcal{K}_0(X) &= \{\widehat{[0] \times [0]}, \widehat{[0] \times [1]}, \widehat{[1] \times [0]}, \widehat{[1] \times [1]}\} \\ \mathcal{K}_1(X) &= \{\widehat{[0] \times [0, 1]}, \widehat{[1] \times [0, 1]}, \widehat{[0, 1] \times [0]}, \widehat{[0, 1] \times [1]}\}. \end{aligned}$$

Now we can compute the boundaries of the elementary cubes.

$$\begin{aligned} \partial_1(\widehat{[0] \times [0, 1]}) &= \widehat{[0] \times [1]} - \widehat{[0] \times [0]} \\ \partial_1(\widehat{[1] \times [0, 1]}) &= \widehat{[1] \times [1]} - \widehat{[1] \times [0]} \\ \partial_1(\widehat{[0, 1] \times [0]}) &= \widehat{[1] \times [0]} - \widehat{[0] \times [0]} \\ \partial_1(\widehat{[0, 1] \times [1]}) &= \widehat{[1] \times [1]} - \widehat{[0] \times [1]}. \end{aligned}$$

The image of  $\partial_0$  is 0 for all  $Q \in \mathcal{K}_0(X)$ .

Remember that  $\widehat{Q \times P} = \widehat{Q} \diamond \widehat{P}$ . We can put the boundary map  $\partial_1$  in form of a matrix

$$\begin{array}{c} \widehat{[0]} \diamond \widehat{[0]} \\ \widehat{[0]} \diamond \widehat{[1]} \\ \widehat{[1]} \diamond \widehat{[0]} \\ \widehat{[1]} \diamond \widehat{[1]} \end{array} \begin{pmatrix} \widehat{[0]} \diamond \widehat{[0, 1]} & \widehat{[1]} \diamond \widehat{[0, 1]} & \widehat{[0, 1]} \diamond \widehat{[0]} & \widehat{[0, 1]} \diamond \widehat{[1]} \\ -1 & 0 & -1 & 0 \\ 1 & 0 & 0 & -1 \\ 0 & -1 & 1 & 0 \\ 0 & 1 & 0 & 1 \end{pmatrix}.$$

To find the 1-cycles of  $X$ , we have to solve the following equation:

$$\begin{pmatrix} -1 & 0 & -1 & 0 \\ 1 & 0 & 0 & -1 \\ 0 & -1 & 1 & 0 \\ 0 & 1 & 0 & 1 \end{pmatrix} \cdot \begin{pmatrix} a \\ b \\ c \\ d \end{pmatrix} = \begin{pmatrix} 0 \\ 0 \\ 0 \\ 0 \end{pmatrix},$$

which gives

$$\begin{pmatrix} -a - c \\ a - d \\ -b + c \\ b + d \end{pmatrix} = \begin{pmatrix} 0 \\ 0 \\ 0 \\ 0 \end{pmatrix}.$$

Thus, we get the solution  $a = -b = -c = d$ , which gives

$$Z_1(X) = \{a(1, -1, -1, 1)^t \mid a \in \mathbb{Z}\}.$$

That means,  $Z_1(X)$  is generated by

$$[\hat{0}] \diamond [\widehat{0,1}] - [\hat{1}] \diamond [\widehat{0,1}] - [\widehat{0,1}] \diamond [\hat{0}] + [\widehat{0,1}] \diamond [\hat{1}].$$

Since there are no 2-cubes in  $X$ , it follows that  $C_2(X) = 0$  and consequently,  $B_1(X) = 0$ . Hence,

$$H_1(X) = Z_1(X) \cong \mathbb{Z}.$$

## 2.4 The Zeroth Homology Group

In this section, we will take a closer look at the zeroth homology group and its topological implications. We will prove that  $H_0(X)$  of a topological space  $X$  is given by the number of connected components  $\text{cc}_X(x)$  of  $X$ , where  $x \in X$ .

**Proposition 2.34** *A cubical set can have only a finite number of connected components.*

**Proof** Every connected component of a cubical set is a connected component of one of its vertices, and a cubical set has only a finite number of vertices.  $\square$

**Definition 2.35** *A sequence of vertices  $v_0, v_1, \dots, v_n \in \mathcal{K}_0(X)$  is an edge path in  $X$  if there exist edges  $e_1, e_2, \dots, e_n \in \mathcal{K}_1(X)$  such that  $v_i, v_{i-1}$  are the two faces of  $e_i$  for  $i = 1, 2, \dots, n$ . For  $v, v' \in \mathcal{K}_0(X)$ , we write  $v \sim_X v'$  if there exists an edge path  $v_0, v_1, \dots, v_n \in \mathcal{K}_0(X)$  in  $X$  such that  $v = v_0$  and  $v' = v_n$ . We say that  $X$  is edge-connected if  $v \sim_X v'$  for any  $v, v' \in \mathcal{K}_0(X)$ . It can be shown easily that  $\sim_X$  is an equivalence relation.*

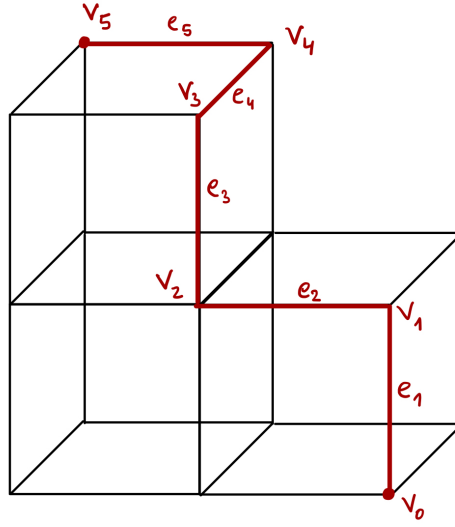


Figure 2.4: An edge path on the union of three elementary cubes

**Example 2.36** In figure 2.4, one can see a cubical set, which is the union of three elementary cubes, and an edge path from the bottom right to the top left  $v_0, v_1, v_2, v_3, v_4, v_5$ . The vertices  $v_i, v_{i-1}$  are the faces of the edge  $e_i$  for  $i = 1, 2, 3, 4, 5$ .

**Proposition 2.37** (i) Every elementary cube is edge-connected.

(ii) If  $X$  and  $Y$  are edge-connected cubical sets and  $X \cup Y \neq \emptyset$ , then  $X \cup Y$  is edge-connected.

**Proof** (i) Let  $X \in \mathcal{K}_k$  for some  $k \in \mathbb{N} \cup \{0\}$ . If  $k = 0$ , then  $X$  is just one vertex, which is edge-connected. For  $k \geq 1$ , we know that  $\mathcal{K}_0(X) \subset \mathcal{K}_1(X)$ . Thus, for every pair of vertices we can find an edge path connecting them.

(ii) It suffices to show that there exists an edge path from  $v_x \in X$  to  $v_y \in Y$ , where  $v_x$  and  $v_y$  are vertices in  $X$  and  $Y$  respectively. Because  $X \cup Y \neq \emptyset$ , there exists at least one vertex  $v$  in the intersection. Therefore,  $v_x \sim_X v$  and  $v_y \sim_X v$ . An edge-path from  $v_x$  to  $v_y$  is given by the composition of the edge-paths  $v_x, \dots, v$  and  $v, \dots, v_y$ . □

**Example 2.38** In Figure 2.5, the union of two edge-connected cubical sets  $X$  and  $Y$  is depicted.

**Proposition 2.39** Assume that  $v \sim_X v'$  for some  $v, v' \in \mathcal{K}_0(X)$ . Then there exists a chain  $c \in C_1(X)$  such that  $|c|$  is connected and  $\partial c = \hat{v}' - \hat{v}$ .

**Proof** Let  $v_0, v_1, \dots, v_n \in \mathcal{K}_0(X)$  be an edge path from  $v = v_0$  to  $v' = v_n$  and let  $e_1, e_2, \dots, e_n \in \mathcal{K}_1(X)$  be the corresponding edges. Without loss of



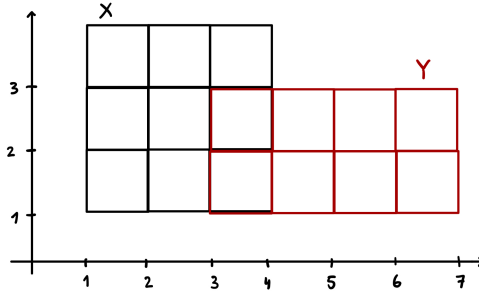


Figure 2.5: The union of two edge-connected cubical sets  $X$  and  $Y$

generality, we may assume that the edge path is minimal. Then any two edges as well as any two vertices in the path are different. We will show that for some coefficients  $\alpha_i \in \{-1, 1\}$  the chain

$$c := \sum_{i=1}^n \alpha_i \hat{e}_i$$

satisfies the conclusions of the proposition. We do so by induction on  $n$ . If  $n = 1$ , then  $\partial e_1 = \pm(\hat{v}_1 - \hat{v}_0)$ . Taking  $c = \alpha_1 \hat{e}_1$  with an appropriate coefficient  $\alpha_1 \in \{-1, 1\}$ , we get  $\partial c = \hat{v}_1 - \hat{v}_0$ . Since  $|c| = |\alpha_1 e_1| = e_1$ , it is connected.

Consider in turn the second step of the induction argument. Let

$$c' := \sum_{i=1}^{n-1} \alpha_i \hat{e}_i$$

with coefficients chosen so that  $\partial c' = \hat{v}_{n-1} - \hat{v}_0$  and  $|c'|$  is connected. Choose  $\alpha_n$  such that  $\partial(\alpha_n e_n) = \hat{v}_n - \hat{v}_{n-1}$ . Then obviously  $\partial c = \hat{v}_n - \hat{v}_0$ . Since  $|c| = |c'| \cup e_n$  and  $|c'| \cap e_n \neq \emptyset$ , it follows that  $|c|$  is connected.  $\square$

**Example 2.40** A chain for the cubical set  $X$  and the edge path in figure 2.4 that fulfills the conditions in proposition 2.39 would be  $c = e_1 + e_2 + e_3 + e_4 + e_5 \in C_1(X)$ . It is clear that  $|c|$  is connected and  $\partial c = v_5 - v_4 + v_4 - \dots - v_1 + v_1 - v_0 = v_5 - v_0$ .

For  $x \in X$  we define the edge-connected component of  $x$  in  $X$  as the union of all edge-connected cubical sets of  $X$  that contain  $x$ . We denote it by  $\text{ecc}_X(x)$ .

**Theorem 2.41** A cubical set  $X$  is connected iff it is edge-connected.

**Proof** Assume first that  $X$  is edge-connected. Let  $v \in X$  be a vertex. It is enough to show that  $\text{cc}_X(v) = X$ , because  $\text{cc}_X(v)$  is connected. Since  $\text{cc}_X(v) \subseteq X$ , we only need to show the opposite inclusion. Thus let  $x \in X$ . Select another vertex  $w \in X$  such that  $x \in \text{cc}_X(x) = \text{cc}_X(w)$ . By proposition

2.39, there exists a chain  $c \in C_1(X)$  such that  $\partial c = \hat{v} - \hat{w}$  and  $|c|$  is connected. Since  $v, w \in |c|$ , it follows that  $\text{cc}_X(w) = \text{cc}_X(v)$ . Therefore,  $x \in \text{cc}_X(v)$ , which we needed to prove.

To prove the opposite implication, assume that  $X$  is not edge-connected. Then there exist vertices  $v_0, v_1 \in \mathcal{K}_0(X)$  such that  $\text{ecc}_X(v_0) \cup \text{ecc}_X(v_1) = \emptyset$ . Let  $X_0 := \text{ecc}_X(v_0)$  and

$$X_1 := \bigcup \{ \text{ecc}_X(v) \mid v \in \mathcal{K}_0(X) \text{ and } \text{ecc}_X(v) \cup \text{ecc}_X(v_0) = \emptyset \}.$$

The sets  $X_0$  and  $X_1$  are disjoint nonempty closed subsets of  $X$ . We will show that  $X = X_0 \cup X_1$ . Let  $x \in X$ . Let  $Q$  be an elementary cube such that  $x \in \mathring{Q}$ . Then  $Q \in X$ . Let  $v \in \mathcal{K}_0(Q)$  by any vertex in  $Q$ . Since by proposition 2.37,  $Q$  is edge-connected,  $Q \subseteq \text{ecc}_X(x)$  and  $Q \subseteq \text{ecc}_X(v)$ . Now if  $\text{ecc}_X(v) = \text{ecc}_X(v_0) = X_0$ , then  $x \in X_0$ . Otherwise,  $x \in X_1$ . This shows that  $X = X_0 \cup X_1$ , which implies that  $X$  is not connected, by contradiction.  $\square$

**Lemma 2.42** *Assume  $X$  is a cubical set and  $X_1, X_2, \dots, X_n$  are its connected components. If  $c_i \in C_k(X_i)$  are  $k$ -dimensional chains, then*

$$\left| \sum_{i=1}^n c_i \right| = \bigcup_{i=1}^n |c_i|.$$

**Proof** The left-hand side is contained in the right-hand side by proposition 2.18 (iv). To show the opposite inclusion, take  $x \in \bigcup_{i=1}^n |c_i|$ . Then for some  $i_0 \in \{1, 2, \dots, n\}$  there exists a  $Q \in \mathcal{K}_k(X_{i_0})$  such that  $x \in Q$  and  $c_{i_0}(Q) \neq 0$ . Since  $Q \notin \mathcal{K}_k(X_j)$  for  $j \neq i_0$ . It follows that

$$\left( \sum_{i=1}^n c_i \right)(Q) = c_{i_0}(Q) \neq 0,$$

that is,  $x \in \left| \sum_{i=1}^n c_i \right|$   $\square$

We can finally prove the main theorem of this section.

**Theorem 2.43** *Let  $X$  be a cubical set. Then  $H_0(X)$  is a free abelian group. Furthermore, if  $\{P_i \mid i = 1, \dots, n\}$  is a collection of vertices in  $X$  consisting of one vertex from each connected component of  $X$ , then*

$$\{[\hat{P}_i] \in H_0(X) \mid i = 1, \dots, n\}$$

*forms a basis for  $H_0(X)$ .*

**Proof** Let  $X_i := \text{cc}_X(P_i)$  and let  $c \in Z_0(X)$ . By proposition 2.39,  $[\hat{P}] = [\hat{P}_i]$  for any  $P \in \mathcal{K}_0(X_i)$ . Since  $Z_0(X) = C_0(X)$ , there exist integers  $\alpha_P$  such that

$$[c] = \sum_{P \in \mathcal{K}_0(X)} \alpha_P [\hat{P}] = \sum_{i=1}^n \sum_{P \in \mathcal{K}_0(X_i)} \alpha_P [\hat{P}] = \sum_{i=1}^n \left( \sum_{P \sim_X P_i} \alpha_P \right) [\hat{P}_i].$$

This shows that the classes  $[\hat{P}_i]$  generate  $H_0(X)$ .  
It remains to show that the generators are free, that

$$\sum_{i=1}^n \alpha_i [\hat{P}_i] = 0$$

implies that all  $\alpha_i = 0$ . To do so, put  $c := \sum_{i=1}^n \alpha_i \hat{P}_i$ . Since  $[c] = 0$ , we can select a  $b \in C_1(X)$  such that  $c = \partial b$ . Let  $b = \sum_{e \in \mathcal{X}_1(X)} \beta_e \hat{e}$ . Let

$$b_i := \sum_{e \in \mathcal{X}_1(X_i)} \beta_e \hat{e}.$$

We have

$$\sum_{i=1}^n \alpha_i \hat{P}_i = c = \partial b = \sum_{i=1}^n \partial b_i.$$

Therefore,

$$0 = \sum_{i=1}^n (\alpha_i \hat{P}_i - \partial b_i).$$

But

$$|\alpha_i \hat{P}_i - \partial b_i| \subseteq X_i.$$

Therefore, by lemma 2.42,

$$\emptyset = |0| = \bigcup_{i=1}^n |\alpha_i \hat{P}_i - \partial b_i|,$$

which shows that  $|\alpha_i \hat{P}_i - \partial b_i| \neq \emptyset$ ; that is, by proposition 2.18 (i),  $\alpha_i \hat{P}_i = \partial b_i$ . Let  $\varepsilon : C_0(X) \rightarrow \mathbb{Z}$  be the group homomorphism defined by  $\varepsilon(\hat{P}) = 1$  for every vertex  $P \in X$ . Let  $e$  be an elementary edge. Then  $\partial \hat{e} = \hat{v}_1 - \hat{v}_0$ , where  $v_0, v_1$  are vertices of  $e$ . Observe that

$$\begin{aligned} \varepsilon(\partial \hat{e}) &= \varepsilon(\hat{v}_1 - \hat{v}_0) \\ &= \varepsilon(\hat{v}_1) - \varepsilon(\hat{v}_0) \\ &= 1 - 1 \\ &= 0. \end{aligned}$$

This implies that  $\varepsilon(\partial b_i) = 0$  and hence

$$0 = \varepsilon(\partial b_i) = \varepsilon(\alpha_i \hat{P}_i) = \alpha_i \varepsilon(\hat{P}_i) = \alpha_i. \quad \square$$

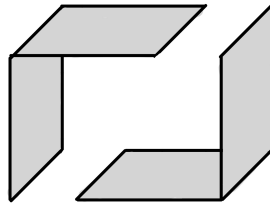


**Figure 2.6:** A cubical set with two connected components.

**Example 2.44** *The cubical set  $X$  in figure 2.6 has two connected components and thus,  $H_0(X)$  is generated by one vertex in each connected component. It follows that  $H_0(X) \cong \mathbb{Z}^2$ .*

## Persistent Homology

In order to analyze images of hurricanes, we can represent the pixels by cubes in integer lattices and apply cubical homology to find patterns in the images. We filter the images by grayscale values to obtain a sequence of binary images, whose homology groups we can then examine using persistent homology. This way, we can track changes in homology in a filtration. By applying the cubical homology functor to a persistent cubical set, we get persistence vector spaces, which we will define in this chapter. We will closely follow the article [1].

**Definition 3.1** A persistent set is a family of sets  $\{X_r\}_{r \in \mathbb{R}}$  together with maps

$$\varphi_r^{r'} : X_r \rightarrow X_{r'} \text{ for all } r \leq r'$$

so that

$$\varphi_r^{r''} \varphi_r^{r'} = \varphi_r^{r''} \text{ for all } r \leq r' \leq r''.$$

**Example 3.2** Let us observe the persistent set  $P$  in Figure 3.1.

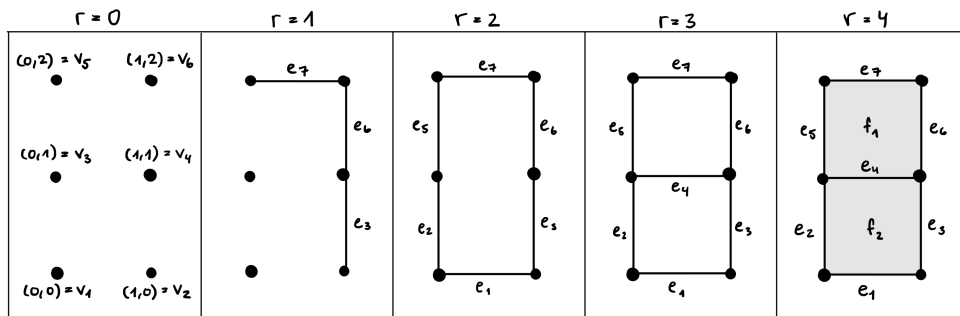


Figure 3.1: The persistent set  $P$ .

At time 0, all of the 0-cubes are added. At time 1, the 1-cubes  $[0, 1] \times [2], [1] \times [1, 2]$  and  $[1] \times [0, 1]$  are added, etc. As in the image, we will continue to write the vertices

as  $v_1, v_2, \dots, v_6$ , the edges as  $e_1, e_2, \dots, e_7$  and the faces as  $f_1$  and  $f_2$  to simplify the notation.

Now we can define persistence vector spaces, that contain within the information about the homology of the cubical sets for every  $R$ , as well as the behaviour of the linear transformations induced by the inclusion maps from one cubical set to another.

**Definition 3.3** Let  $K$  be any field. Then, by a **persistence vector space** over  $K$ , we will mean a family of  $K$ -vector spaces  $\{V_r\}_{r \in \mathbb{R}}$ , together with linear transformations  $L_V(r, r') : V_r \rightarrow V_{r'}$  for  $r \leq r'$ , so that  $L_V(r', r'') \cdot L_V(r, r') = L_V(r, r'')$  for all  $r \leq r' \leq r''$ .

**Definition 3.4** A **linear transformation**  $f$  of persistence vector spaces over  $K$  from  $\{V_r\}$  to  $\{W_r\}$  is a family of linear transformations  $f_r : V_r \rightarrow W_r$ , so that for all  $r \leq r'$ , all the diagrams

$$\begin{array}{ccc} V_r & \xrightarrow{L_V(r, r')} & V_{r'} \\ f_r \downarrow & & \downarrow f_{r'} \\ W_r & \xrightarrow{L_W(r, r')} & W_{r'} \end{array}$$

commute in the sense that  $f_{r'} \circ L_V(r, r') = L_W(r, r') \circ f_r$ .

A **sub-persistence vector space** of  $\{V_r\}$  is a choice of  $K$ -subspaces  $U_r \subseteq V_r$ , for all  $r \in [0, +\infty)$ , so that  $L_V(r, r')(U_r) \subseteq U_{r'}$  for all  $r \leq r'$ . If  $f : \{V_r\} \rightarrow \{W_r\}$  is a linear transformation, then the image of  $f$ , denoted by  $\text{im } f$ , is the sub-persistence vector space  $\{\text{im } f_r\}$ .

**Example 3.5** To compute the homology groups of the persistent set in Example 3.2, we define three persistence vector spaces, which have as a basis the  $i$ -chains for  $i = 0, 1, 2$ , which we denote by  $(C_i(P))_r$ . Generally, persistence vector spaces are over the field  $\mathbb{Z}_2$ , so in computations, we always use  $\mathbb{Z}_2$ -coefficients.

We already saw that all of the vertices are added at time 0. Thus for  $(C_0(P))_r$ , all of the vertices are a basis of the persistence vector space for all  $r \in [0, \infty)$ :

$$(C_0(P))_r = \langle v_1, v_2, v_3, v_4, v_5, v_6 \rangle.$$

We first define the linear maps on the vertices as inclusions and then extend the map linearly to the entire vector space. For the other persistence vector spaces, we get

$$(C_1(P))_r = \begin{cases} 0 & \text{for } r \in [0, 1) \\ \langle e_3, e_6, e_7 \rangle & \text{for } r \in [1, 2) \\ \langle e_1, e_2, e_3, e_5, e_6, e_7 \rangle & \text{for } r \in [2, 3) \\ \langle e_1, e_2, e_3, e_4, e_5, e_6, e_7 \rangle & \text{for } r \in [3, \infty) \end{cases}$$

and

$$(C_2(P))_r = \begin{cases} 0 & \text{for } r \in [0, 3) \\ \langle f_1 \rangle & \text{for } r \in [3, 4) \\ \langle f_1, f_2 \rangle & \text{for } r \in [4, \infty). \end{cases}$$

We can also define a persistence linear map from  $\{(C_i(P))_r\}$  to  $\{(C_{i-1}(P))_r\}$  as a family of cubical boundary maps for  $r \in [0, \infty)$ :

$$(\partial_i)_r : (C_i(P))_r \rightarrow (C_{i-1}(P))_r.$$

The notion of a quotient space also extends to persistence vector spaces. If  $\{U_r\} \subseteq \{V_r\}$  is a sub-persistence vector space, then we can form the persistence vector space  $\{V_r/U_r\}$ , where  $L_{V/U}(r, r')$  is the linear transformation from  $V_r/U_r$  to  $V_{r'}/U_{r'}$  given by sending the equivalence class  $[v]$  to the equivalence class  $[L_V(r, r')(v)]$  for any  $v \in V_r$ .

We extend the notion of a the free vector space on a set:

**Definition 3.6** Let  $X$  be any set, equipped with a function  $\rho : X \rightarrow [0, +\infty)$ . We will refer to such pair as an  $\mathbb{R}_+$ -filtered set. Then, by the free persistence vector space on the pair  $(X, \rho)$ , we will mean the persistence vector space  $\{W_r\}$ , with  $W_r$  equal to the  $K$ -linear span of the set  $X[r] \subseteq X[r']$  when  $r \leq r'$ , so there is an inclusion  $W_r \subseteq W_{r'}$ . Note that  $W_r$  is also contained in the  $K$ -linear span of all elements of  $X$ , which we denote by  $V_K(X)$ .

**Example 3.7** The persistence vector spaces  $C_0(P)_r, C_1(P)_r$  and  $C_2(P)_r$  are free persistence vector spaces, because for  $r \leq r'$  and  $i = 0, 1, 2$ , we have an inclusion  $C_i(P)_r \subseteq C_i(P)_{r'}$ .

Thus, a linear combination  $\sum_x a_x x \in V_K(X)$  lies in  $W_r$ , iff  $a = 0$  for all  $x$  with  $\rho(x) > r$ .

We will write  $\{V_K(X, \rho)_r\}$  for this persistence vector space. We say a persistence vector space is free if it is isomorphic to one of the form  $V_K(X, \rho)$  for some  $(X, \rho)$ , and we say it is finitely generated if  $X$  can be taken to be finite.

**Definition 3.8** A persistence vector space is finitely presented if it is isophormic to a persistence vector space of the form  $\{W_r\} / \text{im } f$  for some linear transformation  $f : \{V_r\} \rightarrow \{W_r\}$  between finitely generated free persistence vector spaces  $\{V_r\}$  and  $\{W_r\}$ .

**Example 3.9**  $P(a, b)$  is a persistence vector space for every pair  $(a, b)$ , where we have  $\infty > a \in \mathbb{R}_+, b \in \mathbb{R}_+, a < b$ , with the obvious interpretation when  $b = \infty$ .  $P(a, b)$  is defined by  $P(a, b)_r = K$  for  $r \in [a, b)$ ,  $P(a, b) = \{0\}$  when  $r \notin [a, b)$ , and where  $L(r, r') = \text{id}_K$  whenever  $r, r' \in [a, b)$ . We note that  $P(a, b)$  is finitely presented. For, in the case where  $b$  is finite, let  $(X, \rho)$  and  $(Y, \sigma)$  denote two  $\mathbb{R}_+$ -filtered sets, with the underlying sets consisting of single elements  $x$  and  $y$ , and with  $\rho(x) = a$  and  $\sigma(y) = b$ . Then the  $(1 \times 1)(X, Y)$ -matrix  $[1]$  is  $(\rho, \sigma)$ -adapted since

$a \leq b$  and it is clear that  $P(a, b)$  is isomorphic to  $\theta([1])$ . When  $b = \infty$ ,  $P(a, b)$  is isomorphic to the persistence vector space  $V_k(X, \rho)$ , and can therefore be written as  $\theta(0)$ , where  $0$  denotes the zero linear transformation from the persistence vector space  $\{0\}$ .

The choice of a basis for vector spaces  $V$  and  $W$  allow us to represent linear transformations from  $V$  to  $W$  by matrices. For any pair  $(X, Y)$  of finite sets and field  $K$ , an  $(X, Y)$ -matrix is an array  $[a_{xy}]$  of elements of  $a_{xy}$  of  $K$ . We write  $r(x)$  for the row corresponding to  $x$  and  $c(y)$  for the column corresponding to  $y$ . For any finitely generated free persistence vector space  $\{V_r\} = \{V_K(X, \rho)_r\}$ , we observe that  $V_K(X, \rho)_r = V_K(X)$  for  $r$  sufficiently large, since  $X$  is finite.

Therefore, for any linear transformation  $f : \{V_K(Y, \rho)_r\} \rightarrow \{V_K(X, \rho)_r\}$  of finitely generated free persistence vector spaces,  $f$  gives a linear transformation  $f_\infty : V_K(X) \rightarrow V_K(Y)$  between finite-dimensional vector spaces over  $K$ , and using the bases  $\{\varphi_x\}_{x \in X}$  of  $V_K(X)$  and  $\{\varphi_y\}_{y \in Y}$  of  $V_K(Y)$  determines an  $(X, Y)$ -matrix  $A(f) = [a_{xy}]$  with entries in  $K$ . So, labels for the rows and columns play an important role, as they are the basis elements of  $V_K(X)$  and  $V_K(Y)$ .

**Proposition 3.10** *The  $(X, Y)$ -matrix  $A(f)$  has the property that  $a_{xy} = 0$  whenever  $\rho(x) > \sigma(y)$ . Any  $(X, Y)$ -matrix  $A$  satisfying this condition uniquely determines a linear transformation of persistence vector spaces*

$$f_A : \{V_K(Y, \sigma)_r\} \rightarrow \{V_K(X, \rho)_r\}$$

and the correspondences  $f \rightarrow A(f)$  and  $A \rightarrow f_A$  are inverses to each other.

**Proof** The basis vector  $y$  lies in  $V_K(Y, \sigma)_{\sigma(y)}$ . On the other hand,

$$f(\varphi_y) = \sum_{x \in X} a_{xy} \varphi_x.$$

On the other hand,  $\sum_{x \in X} a_{xy} \varphi_x$  only lies in  $V_K(X, \rho)_{\sigma(y)}$  if all coefficients  $a_{xy}$ , for  $\rho(x) > \sigma(y)$ , are zero. □

**Definition 3.11** *An  $(X, Y)$ -matrix of a pair of  $\mathbb{R}_+$ -filtered finite sets  $(X, \rho)$  and  $(Y, \sigma)$  which satisfies the condition in proposition 3.10, i.e.  $a_{xy} = 0$  whenever  $\rho(x) > \sigma(y)$ , is  $(\rho, \sigma)$ -adapted.*

**Example 3.12** *If we take a look at the persistent set of Example 3.2, we can write down the  $(\rho, \sigma)$ -adapted matrices  $\partial_1$  and  $\partial_2$ .*



$$\begin{array}{c}
(v_{1,0}) \\
(v_{2,0}) \\
(v_{3,0}) \\
(v_{4,0}) \\
(v_{5,0}) \\
(v_{6,0})
\end{array}
\begin{pmatrix}
(e_{1,2}) & (e_{2,2}) & (e_{3,1}) & (e_{4,3}) & (e_{5,2}) & (e_{6,1}) & (e_{7,1}) \\
1 & 1 & 0 & 0 & 0 & 0 & 0 \\
1 & 0 & 1 & 0 & 0 & 0 & 0 \\
0 & 1 & 0 & 1 & 1 & 0 & 0 \\
0 & 0 & 1 & 1 & 0 & 1 & 0 \\
0 & 0 & 0 & 0 & 1 & 0 & 1 \\
0 & 0 & 0 & 0 & 0 & 1 & 1
\end{pmatrix},
\begin{array}{c}
(e_{1,2}) \\
(e_{2,2}) \\
(e_{3,1}) \\
(e_{4,3}) \\
(e_{5,2}) \\
(e_{6,1}) \\
(e_{7,1})
\end{array}
\begin{pmatrix}
(f_{1,4}) & (f_{2,4}) \\
0 & 1 \\
0 & 1 \\
0 & 1 \\
1 & 1 \\
1 & 0 \\
1 & 0 \\
1 & 0
\end{pmatrix}$$

A  $(\rho, \sigma)$ -adapted matrix  $A = [a_{xy}]$  determines a persistence vector space via the correspondence

$$A \xrightarrow{\theta} V_k(X, \rho) / \text{im } f_A.$$

$\theta$  has the following properties:

**Corollary 3.13** *Let  $(X, \rho)$  and  $(Y, \sigma)$  be  $\mathbb{R}_+$ -filtered sets.*

- (i)  $\theta(A)$  is a finitely presented vector space. Moreover, any finitely presented persistent vector space is isomorphic to one of the form  $\theta(A)$  for some matrix  $A$ .
- (ii) Under the matrix-linear-transformation correspondence, the automorphisms of  $V_k(X, \rho)$  are identified with the group of all invertible  $(\rho, \rho)$ -adapted  $(X, X)$ -matrices.
- (iii) Let  $A$  be a  $(\rho, \sigma)$ -adapted,  $B$  be a  $(\rho, \rho)$ -adapted and  $C$  be a  $(\sigma, \sigma)$ -adapted matrix. Then  $BAC$  is also  $(\rho, \sigma)$ -adapted, and the persistence vector space  $\theta(A)$  is isomorphic to  $\theta(BAC)$ .

We will use these results to classify up to isomorphism all finitely presented persistence vector spaces.

**Proposition 3.14** *Every finitely presented persistence vector space over  $K$  is isomorphic to a finite direct sum of the form*

$$P(a_1, b_1) \oplus P(a_2, b_2) \oplus \dots \oplus P(a_n, b_n)$$

for some choices  $a_i \in [0, +\infty)$ ,  $b_i \in [0, +\infty]$ , and  $a_i < b_i$  for all  $i$ .

**Proof** It is clear that a  $(\rho, \sigma)$ -adapted  $(X, Y)$ -matrix  $A$  which has the property that every row and column has at most one nonzero element, which is equal to 1, has the property that  $\theta(A)$  is of the form described in the proposition. For if we let  $\{(x_1, y_1), (x_2, y_2), \dots, (x_n, y_n)\}$  be all the pairs  $(x_i, y_i)$ , so that  $a_{x_i, y_i} = 1$ , then there is a decomposition

$$\theta(A) \cong \bigoplus_i P(\rho(x_i), \sigma(y_i)) \oplus \bigoplus_{x \in X - \{x_1, \dots, x_n\}} P(\rho(x), +\infty). \quad (3.1)$$

So, it suffices to construct matrices  $B$  and  $C$ , that are  $(\rho, \rho)$ -adapted (respectively  $(\sigma, \sigma)$ -adapted)  $(X, X)$ -matrices (respectively  $(Y, Y)$ -matrices), so that  $BAC$  has the property that every row and column has at most one nonzero element, which is 1. To see this, we define  $(\rho, \sigma)$ -adapted row and column operations, which consist of:

- (i) all possible multiplications of a row and column by a nonzero element,
- (ii) all possible additions of a multiple of  $r(x)$  to  $r(x')$  when  $\rho(x) \geq \rho(x')$ ,
- (iii) all possible additions of a multiple of  $c(y)$  to  $c(y')$  when  $\sigma(y) \leq \sigma(y')$ .

Because we observe pairs of matrices  $(A, B)$  with  $A \cdot B = 0$  (in our case, these will be two consecutive boundary maps), we have the following admissible operations on such pair:

- (i) An arbitrary adapted row operation on  $A$ ,
- (ii) An arbitrary column operation on  $B$ ,
- (iii) Perform an adapted column operation on  $A$  and an adapted row operation on  $B$  simultaneously, with the operations related as follows. If the adapted column operation on  $A$  is the multiplication of the  $i$ th column by a nonzero constant  $a$ , then the adapted row operation on  $B$  is the multiplication of the  $i$ th row by  $a^{-1}$ . If the adapted column operation on  $A$  is the transposition of two columns, then the adapted row operation on  $B$  is the transposition of the corresponding rows of  $B$ . Finally, if the adapted column operation on  $A$  is the addition of  $x$  times the  $i$ th column to the  $j$ th column, then the adapted row operation on  $B$  is the subtraction of  $x$  times the  $j$ th row from the  $i$ th row.

*Claim:* By performing  $(\rho, \sigma)$ -adapted row and column operations, we can arrive at a matrix with at most one nonzero entry in each row and column.

*proof of claim:* First find a  $y$  which minimizes  $\sigma(y)$  over the set of all  $y$  with  $c(y) \neq 0$ . Next, find an  $x$  which maximizes  $\rho(x)$  over the set of all  $x$  for which the entry  $a_{xy} \neq 0$ .

Because of the way  $x$  is chosen, we can add multiples of  $r(x)$  to all the other rows so as to 'zero out'  $c(y)$  except in the  $xy$ -entry. Because of the way  $y$  is chosen, we can add multiples of  $c(y)$  to zero out  $r(x)$  except in the  $xy$ -entry, without affecting  $c(y)$ .

The result is a matrix in which the unique nonzero element in both  $r(x)$  and  $c(y)$  is  $a_{xy}$ . By multiplying  $r(x)$  by  $\frac{1}{a_{xy}}$ , we can make the  $xy$ -entry in the transformed matrix 1. By deleting  $r(x)$  and  $c(y)$ , we obtain a  $(X - \{x\}, Y - \{y\})$ -matrix which is  $(\rho|_{X - \{x\}}, \sigma|_{Y - \{y\}})$ -adapted.

We can now apply the process inductively to the matrix. Each of the row and column operations required can be interpreted as row and column operations on the original matrix, and will have no effect on  $r(x)$  or  $c(y)$ .

The result is that by iterating this procedure, we will eventually arrive at a

matrix with only zero entries, and it is clear that the transformed matrix has at most one nonzero element in each row and column. The result follows by (iii) of corollary 3.13.  $\square$

This proposition gives us an algorithm to compute the persistent homology of a persistent vector space. It is only left to show that the decomposition given in the proposition is unique.

**Proposition 3.15** *Suppose that  $\{V_r\}$  is a finitely presented persistence vector space over  $K$ , and that we have two decompositions*

$$\{V_r\} \cong \bigoplus_{i \in I} P(a_i, b_i) \text{ and } \{V_r\} \cong \bigoplus_{j \in J} P(c_j, d_j),$$

where  $I$  and  $J$  are finite sets. Then  $\#(I) = \#(J)$ , and the set of pairs  $(a_i, b_i)$  is, with multiplicities, identical to the set of pairs  $(c_j, d_j)$ .

**Proof** We let  $a_{min}$  and  $c_{min}$  denote the smallest value of  $a_i$  and  $c_j$ , respectively.  $a_{min}$  can be characterized intrinsically as  $\min\{r | V_r \neq 0\}$ , and it follows that  $a_{min} = c_{min}$ .

Next, let  $b_{min}$  denote  $\min\{b_i | a_i = a_{min}\}$ , and make the corresponding definition for  $d_{min}$ .  $b_{min}$  is also defined intrinsically as  $\min\{r' | N(L(r, r')) \neq 0\}$ , where  $N$  denotes the null space, so  $b_{min} = d_{min}$  as well. This means that  $P(a_{min}, b_{min})$  appears in both decompositions.

For each decomposition, we consider the sum of all occurrences of the summand  $P(a_{min}, b_{min})$ . They are both sub-persistence vector spaces of  $\{V_r\}$ , and can in fact be characterized intrinsically as the sub-persistence vector space  $\{W_r\}$ , where  $W_r$  is the null space of the linear transformation

$$\text{im } L(a_{min}, r) \xrightarrow{L(r, b_{min})|_{\text{im } L(a_{min}, r)}} V_{b_{min}}.$$

It now follows that the number of summands of the form  $P(a_{min}, b_{min})$  in the two decompositions are the same, and further that they correspond isomorphically under the decompositions.

Let  $I'$  denote the subset of  $I$  obtained by removing all  $i$  so that  $a_i = a_{min}$  and  $b_i = b_{min}$ , and define  $J'$  correspondingly. We can now form the quotient of  $\{V_r\}$  by  $\{W_r\}$ , and observe that we obtain identifications

$$\{V_r\} / \{W_r\} \cong \bigoplus_{i \in I'} P(a_i, b_i) \text{ and } \{V_r\} / \{W_r\} \cong \bigoplus_{j \in J'} P(c_j, d_j).$$

By induction on the number of summands in the decompositions, we obtain the result.  $\square$

**Example 3.16** *Using the algorithm given in the proof of proposition 3.14, we can compute the persistent homology groups of the persistent set in Example 3.2 by*

### 3. PERSISTENT HOMOLOGY

applying  $(\rho, \sigma)$ -adapted row and column operations to the matrix  $(\partial_1, \partial_2)$  to get a pair of matrices which have diagonal blocks. First, we order the columns of  $\partial_1$  by ascending  $\sigma(e_i)$  for  $i = 1, \dots, 7$  and then sort the rows of  $\partial_2$  accordingly.

$$\left( \begin{array}{cccc|ccc} (e_3,1) & (e_6,1) & (e_7,1) & (e_1,2) & (e_2,2) & (e_5,2) & (e_4,3) & (e_3,1) & (f_1,4) & (f_2,4) \\ \left( \begin{array}{cccc} 0 & 0 & 0 & 1 \\ 1 & 0 & 0 & 1 \\ 0 & 0 & 0 & 0 \\ 1 & 1 & 0 & 0 \\ 0 & 0 & 1 & 0 \\ 0 & 1 & 1 & 0 \end{array} \right) & & & & & & & \left( \begin{array}{cc} 0 & 1 \\ 1 & 0 \\ 1 & 0 \\ 0 & 1 \\ 0 & 1 \\ 1 & 0 \\ 1 & 1 \end{array} \right) \end{array} \right)$$

Next, we exchange  $r(1)$  and  $r(2)$  of  $\partial_1$  to get a 1 in the top-left entry.

$$\left( \begin{array}{cccc|ccc} (e_3,1) & (e_6,1) & (e_7,1) & (e_1,2) & (e_2,2) & (e_5,2) & (e_4,3) & (e_3,1) & (f_1,4) & (f_2,4) \\ \left( \begin{array}{cccc} 1 & 0 & 0 & 1 \\ 0 & 0 & 0 & 1 \\ 0 & 0 & 0 & 0 \\ 1 & 1 & 0 & 0 \\ 0 & 0 & 1 & 0 \\ 0 & 1 & 1 & 0 \end{array} \right) & & & & & & & \left( \begin{array}{cc} 0 & 1 \\ 1 & 0 \\ 1 & 0 \\ 0 & 1 \\ 0 & 1 \\ 1 & 0 \\ 1 & 1 \end{array} \right) \end{array} \right)$$

In order to eliminate the other 1 in  $r(1)$  of  $\partial_1$ , we add  $r(1)$  to  $r(4)$ . Because the row labels are all 0, we can add and subtract them as we wish.

$$\left( \begin{array}{cccc|ccc} (e_3,1) & (e_6,1) & (e_7,1) & (e_1,2) & (e_2,2) & (e_5,2) & (e_4,3) & (e_3,1) & (f_1,4) & (f_2,4) \\ \left( \begin{array}{cccc} 1 & 0 & 0 & 1 \\ 0 & 0 & 0 & 1 \\ 0 & 0 & 0 & 0 \\ 0 & 1 & 0 & 1 \\ 0 & 0 & 1 & 0 \\ 0 & 1 & 1 & 0 \end{array} \right) & & & & & & & \left( \begin{array}{cc} 0 & 1 \\ 1 & 0 \\ 1 & 0 \\ 0 & 1 \\ 0 & 1 \\ 1 & 0 \\ 1 & 1 \end{array} \right) \end{array} \right)$$

To get rid of the other 1 in  $c(1)$  of  $\partial_1$ , we add  $c(1)$  to  $c(4)$ . Because we can only apply adapted row and column operations, we have to add  $r(4)$  of  $\partial_2$  to  $r(1)$  and adjust the labels of the columns of  $\partial_1$  and the rows of  $\partial_2$ .

$$\left( \begin{array}{cccc|ccc} (e_3,1) & (e_6,1) & (e_7,1) & (e_1e_3,2) & (e_2,2) & (e_5,2) & (e_4,3) & (e_3,1) & (f_1,4) & (f_2,4) \\ \left( \begin{array}{cccc} 1 & 0 & 0 & 0 \\ 0 & 0 & 0 & 1 \\ 0 & 0 & 0 & 0 \\ 0 & 1 & 0 & 1 \\ 0 & 0 & 1 & 0 \\ 0 & 1 & 1 & 0 \end{array} \right) & & & & & & & \left( \begin{array}{cc} 0 & 0 \\ 1 & 0 \\ 1 & 0 \\ 0 & 1 \\ 0 & 1 \\ 1 & 0 \\ 1 & 1 \end{array} \right) \end{array} \right)$$

Now, the first row and column of  $\partial_1$  are in the desired form and we can apply the same steps to the bottom-right  $5 \times 6$ -submatrix and so on. After we put  $\partial_1$  in a diagonal form, we can apply column operations to  $\partial_2$  to obtain a diagonal submatrix in the bottom-right. In the end, we obtain

$$\left( \begin{array}{cccc|ccc} (e_3,1) & (e_6,1) & (e_7,1) & (e_1e_3e_6,2) & (e_1e_2e_3e_6,2) & (e_1e_2e_3e_5e_6e_7,2) & (e_1e_2e_3e_4,3) & (e_3,1) & (f_1f_2,4) & (f_2,4) \\ \left( \begin{array}{cccc} 1 & 0 & 0 & 0 \\ 0 & 1 & 0 & 0 \\ 0 & 0 & 1 & 0 \\ 0 & 0 & 0 & 1 \\ 0 & 0 & 0 & 0 \\ 0 & 0 & 0 & 0 \end{array} \right) & & & & & & & \left( \begin{array}{cc} 0 & 0 \\ 0 & 0 \\ 0 & 0 \\ 0 & 0 \\ 1 & 0 \\ 0 & 1 \end{array} \right) \end{array} \right)$$

To shorten the notation, we omitted the plus sign in the labels. We observe that  $\partial(f_1 + f_2) = e_1 + e_2 + e_3 + e_5 + e_6 + e_7$  and  $\partial(f_2) = e_1 + e_2 + e_3 + e_4$ . From the matrix on the left we can now read off that the persistence vector space  $\ker \partial_1$  is isomorphic to  $(X, \rho)$ , where  $X = \{\partial(f_1 + f_2), \partial(f_2)\}$  and  $\rho(\partial(f_1 + f_2)) = 2$ ,  $\rho(\partial(f_2)) = 3$ . To get the 1-dimensional persistent homology group, we observe the persistence linear map  $(\partial_2)_r : (C_2(P))_r \rightarrow (\ker \partial_1)_r$ ,  $r \in [0, \infty)$ . This map is represented by the following  $(\{\partial(f_1 + f_2), \partial(f_2)\}, \{f_1 + f_2, f_2\})$ -adapted matrix

$$\begin{matrix} & \begin{matrix} (f_1 + f_2, 4) & (f_2, 4) \end{matrix} \\ \begin{matrix} (\partial(f_1 + f_2), 2) \\ (\partial(f_2), 3) \end{matrix} & \begin{pmatrix} 1 & 0 \\ 0 & 1 \end{pmatrix} \end{matrix}$$

According to Proposition 3.14, the 1-dimensional persistent homology group is isomorphic to  $P(2, 4) \oplus P(3, 4)$ . Since we retained the information about how the basis changed, we can read off what the cycles are:  $\partial(f_1 + f_2)$  persists over  $[2, 4)$  and  $\partial(f_2)$  persists over  $[3, 4)$ .

The isomorphism classes of finitely presented persistence vector spaces are in one-to-one correspondence with the set  $\{(a, b) | a \in [0, \infty), b \in [0, \infty], a < b\}$ . Such sets can be represented visually in two distinct ways, one as families of intervals on the non-negative real lines, and the other as a collection of points in the subset  $\{(x, y) | x \geq 0 \text{ and } y > x\}$  of the first quadrant in the  $(x, y)$ -plane. In the second case, one must place points with  $b = +\infty$  above the whole diagram in a horizontal line indicating infinity. The first representation is called a barcode, the second a persistence diagram.

Usually, the persistence barcodes consist of some ‘short’ intervals and some ‘long’ intervals. The short intervals are typically considered noisy, whereas the long ones are considered to correspond to larger-scale geometric features, which one would expect to have a correspondence with the features of a space from which the metric is sampled.

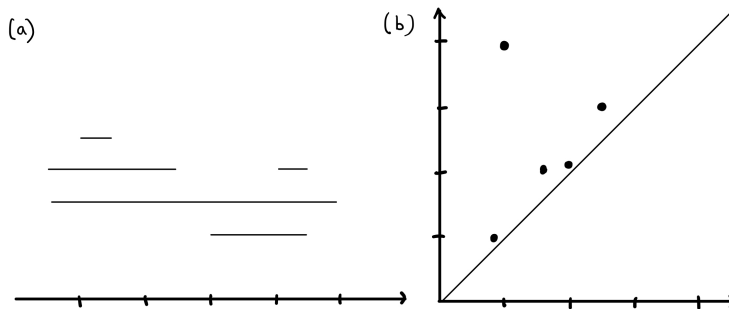


Figure 3.2: (a) a barcode; (b) a persistence diagram

**Definition 3.17** The lifetime of  $P(a_i, b_i)$  is  $b_i - a_i$  [5].

### 3. PERSISTENT HOMOLOGY

In the persistence diagram, a long lifetime of  $P(a_i, b_i)$  would be represented by a point far from the diagonal axis, whereas a short lifetime would be represented by a point close to the diagonal axis.

**Definition 3.18** The maximum persistence  $\text{MaxPers}(D) := \max_{(a_i, b_i) \in D} (b_i - a_i)$  for a given persistence diagram  $D$  measures the longest lifetime of a space  $P(a_i, b_i)$  in the diagram.

**Example 3.19** As an example, we take a look at Figure 3.3<sup>1</sup>, which shows an image of a circle. We first convert the image into a cubical complex: there are  $8 \times 8$  elementary 2-cubes, and to every 2-cube there is a value assigned to it, which can be seen as the ‘time’  $r$ , the 2-cube (and all its faces) appears in the persistence vector space  $\{V_r\}_r$ . This value is also the greyscale value of the color of the 2-cube. Because the image is an image of a circle, persistent homology should yield the homology groups of a circle (or a shape that is homotopy equivalent).

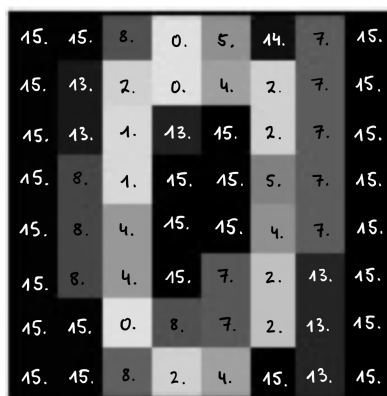


Figure 3.3:  $8 \times 8$  grayscale image of a circle

Now we apply persistent homology to compute the barcodes of the image. We want to focus on computing  $H_1$  (Because  $H_0$  is just the number of path-connected components). We recall from example 2.33, that  $H_1 \cong \mathbb{Z}$ .

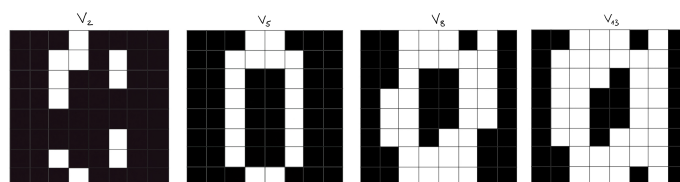
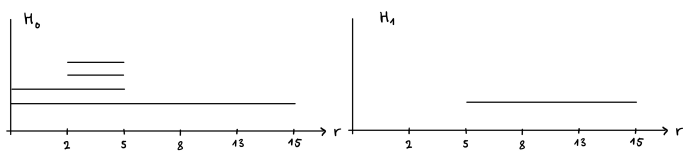


Figure 3.4: The vector space  $V_r$  for different  $r$ 's

<sup>1</sup>[https://scikit-learn.org/stable/auto\\_examples/cluster/plot\\_digits\\_agglomeration.html#sphx-glr-auto-examples-cluster-plot-digits-agglomeration-py](https://scikit-learn.org/stable/auto_examples/cluster/plot_digits_agglomeration.html#sphx-glr-auto-examples-cluster-plot-digits-agglomeration-py); last access 19.06.2023

---

In Figure 3.4, one can see the vector spaces  $V_2$ ,  $V_5$ ,  $V_8$  and  $V_{13}$ . In  $V_2$ , there are 4 path-connected components, but circle-like shape is not visible yet. In  $V_5$  the circle-like shape is visible for the first time and it continues to be visible until  $V_{15}$ . The barcode for  $H_1$  is depicted in figure 3.5.



**Figure 3.5:** The barcodes for  $H_0$  and  $H_1$





---

# Topological Analysis of Tropical Cyclones

---

Previous studies described that hurricanes have a diurnal cycle [2],[7], which can be observed in infrared satellite imagery as distinct pulses that expand radially outward. These pulses may influence the structure and intensity of the hurricane. Thus understanding them better could help to improve weather forecasting or security measures. Despite this, there is little quantitative research available that concerns this phenomenon.

In [5], a method based on persistent homology is used to analyze the diurnal cycle of hurricanes. Because the aim is to capture cycles in the data, the first homology group, which in this case should be non-trivial, plays an important role.

## 4.1 Tropical Cyclone Formation & Diurnal Cycles

The term tropical cyclone (TC) includes hurricanes, typhoons and cyclones. Generally, tropical cyclones are called hurricanes if they are in the Atlantic, typhoons if they are in the Pacific and cyclones if they are in the Indian Ocean [7].

The main condition for the formation of a TC is a large, still and warm ocean area with a surface temperature over 26 to 27 °C. As a consequence, a body of warm air forms over the water, rises and forms clouds beyond the condensation level. During that process, latent heat energy is released which leads to a self-sustaining heat cycle. Due to the Coriolis effect currents of air spiral around the center of the TC. Thus, they rotate anti-clockwise in the northern hemisphere and clockwise in the southern hemisphere. The pressure is lowest in the center of the TC and increases radially outward.

At this stage, the TC is matured and follows a pathway away from its source driven by global wind circulation.

#### 4. TOPOLOGICAL ANALYSIS OF TROPICAL CYCLONES

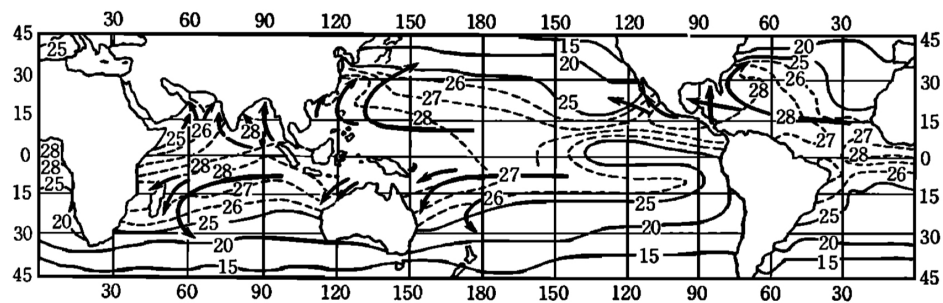


**Figure 4.1:** Principal tropical cyclone paths and sea surface temperature during summer season (for both hemispheres)(image taken from [7])

As the reader can derive from Figure 4.1, the latent energy distribution varies with location, but also with season.

Previous research documented a diurnal cycle of tropical convection and the tropical cyclone cirrus canopy, which are the upper-level clouds of the hurricane. They found a distinct pulse in the investigated storms that begins around the time of the local sunset, forms in the core of the TC and expands outward radially, reaching the periphery of the hurricane in the early afternoon [2], which can also be observed in satellite data. These pulses may have implications for the structure and intensity of the TC, as they propagate ‘through a deep layer of TC environment’ [5].

The cirrus canopy expands as well throughout the day, reaching the maximal area coverage in the early evening hours [5]. Moreover, convection such as thunderstorms occur overnight and precipitation peaks near sunrise [5]. In general, research ‘suggests that the TC diurnal cycle favors storm intensification in the early hours of the morning and storm weakening in the late afternoon and evening’ [4]. Also, this outward propagating pulse has been found in 88 % of all hurricanes between 1982 and 2017 in the Atlantic ocean, thus one can say that this is a ubiquitous phenomenon.

But it is not yet understood why there is a diurnal cycle, what the dynamical mechanisms and what the impact to the storm structure and intensity are [4]. It is suspected that the phenomenon may have something to do with solar radiation [5],[2]. The main source of this thesis takes another approach to examine and quantify the diurnal cycle by using persistent homology.

## 4.2 Analysis of Tropical Cyclones using Persistent Homology

Before we begin with the topological analysis of TCs, we need to take a closer look at the discrete Fourier transform, which is used in the method presented in [5]. I will refer to [6] and [5].

As with the continuous Fourier transformation, the discrete Fourier transformation (DFT) is used to decompose a (discrete) function  $f$  into a sum of sinuoids with different frequencies [5]. Let  $N$  be the number of samples,  $T$  be the time between the discrete samples and let  $t_k = kT$ , where  $k = 0, \dots, N - 1$ .

The result of the transformation is a vector  $F = (F_0, \dots, F_{N-1}) \in \mathbb{C}^N$ , where the  $F_0, \dots, F_{N-1}$  are the Fourier coefficients. These are given by

$$F_n := \sum_{k=0}^{N-1} f(t_k) e^{-2\pi i n k / N}. \quad (4.1)$$

The sum of the sinuoids, which have amplitude  $F_n$  for  $n = 0, \dots, N - 1$ , gives the original function  $f$ . Thus for the inverse DFT, we get the equation

$$f(t_k) = \frac{1}{N} \sum_{j=0}^{N-1} F_j e^{2\pi i j k / N}. \quad (4.2)$$

The power in each frequency component represented by the DFT is  $|F_n|^2$  and can be used to find the most dominant frequency in the function  $f$ .

**Example 4.1** *Let's consider the following example: take*

$$f(0) = 1, f(2) = 4, f(4) = 3, f(6) = 2.$$

*Clearly,  $T = 2$  and  $N = 4$ . We can now compute the Fourier coefficients with equation 4.1.*

$$\begin{aligned} F_0 &= f(0)e^{-2\pi i \cdot 0 \cdot 0/4} + f(2)e^{-2\pi i \cdot 0 \cdot 1/4} + f(4)e^{-2\pi i \cdot 0 \cdot 2/4} + f(6)e^{-2\pi i \cdot 0 \cdot 3/4} \\ &= 1 + 4 + 3 + 2 = 10 \end{aligned}$$

$$\begin{aligned} F_1 &= f(0)e^{-2\pi i \cdot 1 \cdot 0/4} + f(2)e^{-2\pi i \cdot 1 \cdot 1/4} + f(4)e^{-2\pi i \cdot 1 \cdot 2/4} + f(6)e^{-2\pi i \cdot 1 \cdot 3/4} \\ &= 1 + 4e^{-\pi i/2} + 3e^{-\pi i} + 2e^{-3\pi i/2} \\ &= 1 - 4i - 3 + 2i = -2 - 2i \end{aligned}$$

$$\begin{aligned} F_2 &= f(0)e^{-2\pi i \cdot 2 \cdot 0/4} + f(2)e^{-2\pi i \cdot 2 \cdot 1/4} + f(4)e^{-2\pi i \cdot 2 \cdot 2/4} + f(6)e^{-2\pi i \cdot 2 \cdot 3/4} \\ &= 1 + 4e^{-\pi i} + 3e^{-2\pi i} + 2e^{-3\pi i} \\ &= 1 - 4 + 3 - 2 = -2 \end{aligned}$$

$$\begin{aligned} F_3 &= f(0)e^{-2\pi i \cdot 3 \cdot 0/4} + f(2)e^{-2\pi i \cdot 3 \cdot 1/4} + f(4)e^{-2\pi i \cdot 3 \cdot 2/4} + f(6)e^{-2\pi i \cdot 3 \cdot 3/4} \\ &= 1 + 4e^{-3\pi i/2} + 3e^{-3\pi i} + 2e^{-9\pi i/2} \\ &= 1 + 4i - 3 - 2i = -2 + 2i \end{aligned}$$

#### 4. TOPOLOGICAL ANALYSIS OF TROPICAL CYCLONES

The absolute value of the Fourier coefficients give us the amplitude of the corresponding sinusoid and  $f$  is given by

$$\begin{aligned} f(t_k) &= \frac{1}{4}(10e^{2\pi i \cdot 0 \cdot k/4} - (2+2i)e^{2\pi i \cdot 1 \cdot k/4} - 2e^{2\pi i \cdot 2 \cdot k/4} - (2-2i)e^{2\pi i \cdot 3 \cdot k/4}) \\ &= \frac{1}{4}(10 - (2+2i)e^{\pi i k/2} - 2e^{\pi i k} - (2-2i)e^{3\pi i k/2}) \end{aligned}$$

Thus, we see that the sinusoid corresponding to  $F_0$  has the biggest amplitude, which is the constant function  $g(t_k) = 10e^{2\pi i \cdot 0 \cdot k/4} = 10$ . Since the computation is very tedious if done by hand, computers are used to compute the DFT.

Sarah Tymochko et al. used persistent homology to quantify the diurnal cycle. All the images in the following section are taken from [5]. The data used was Geostationary Operational Environmental Satellite (GOES) infrared (IR) satellite data, which can ‘detect clouds at all times of the day and night and is ideal for tracing the evolution of the TC cloud fields’, for the hurricanes Felix in 2007 and Ivan in 2004. The data was given in hourly time increments, represented as a matrix for pixel values  $S(t)$  for time  $t$ , similarly as in Example 3.19. One exemplary satellite image can be seen in Figure 4.2.

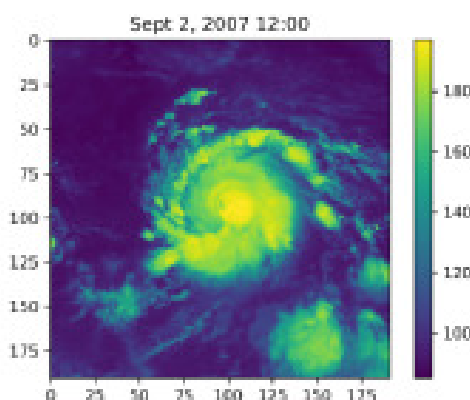


**Figure 4.2:** Original satellite imagery from the Felix data set

To detect the movement and changes in the brightness temperature, the six-hour-differences  $M(t) = S(t+6) - S(t)$  was considered for all times  $t$  and a threshold  $\mu$  was fixed to define  $M(t)_\mu$ , which is the subset of  $M(t)$  with function value less than  $\mu$ . Thus,  $M(t)_\mu[i, j] = 1$  if  $M(t)[i, j] < \mu$  and  $M(t)_\mu[i, j] = 0$  otherwise. Because  $M(t)$  is the difference of two images, the threshold  $\mu$  isolates all the pixels that increase by  $\mu$  over the six hours.

After, the distance transform  $D(t)$  of  $M(t)$  was computed to create a greyscale image that ‘maintains the visually apparent topological structure of the image’. The distance transform is a matrix which is calculated componentwise:

## 4.2. Analysis of Tropical Cyclones using Persistent Homology

$D(t)_{i,j} = \min_{i,j} d_\infty(s_{i,j}, x)$ , where  $s_{i,j}$  is the pixel at  $(i, j)$  and

$$d_\infty(s_{i_1, j_1}, s_{i_2, j_2}) = \max\{|i_2 - i_1|, |j_2 - j_1|\}$$

is the  $L_\infty$ -distance between  $s_{i_1, j_1}$  and  $s_{i_2, j_2}$ .

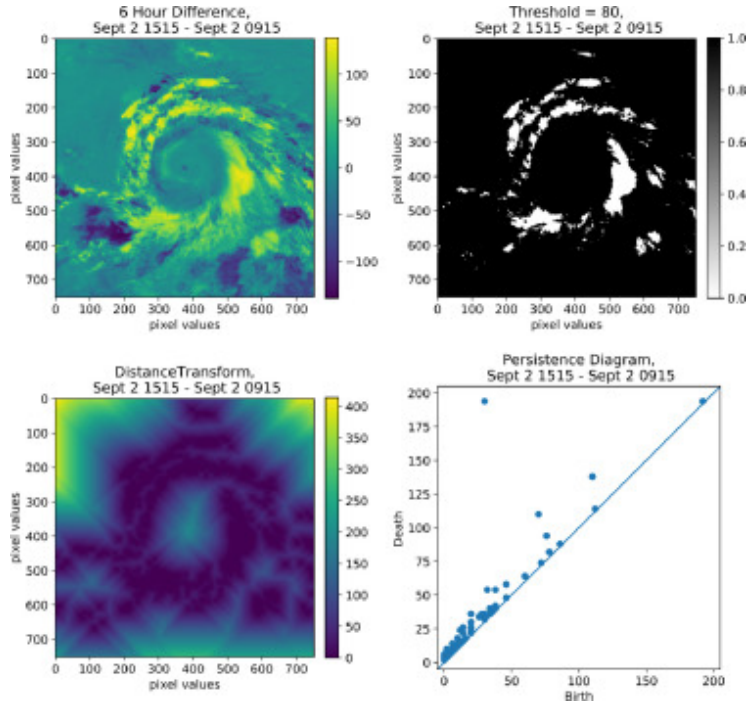


**Figure 4.3:** Top left: Example of six-hour-difference  $M(t)$  from the Felix data set; Top right: thresholded subset  $M(t)_\mu$  with  $\mu = 80$ ; Bottom left: distance transform  $D(t)$ ; Bottom right: corresponding persistence diagram

Then, the persistent homology of the cubical set on the function  $D(t)$  was computed for every six-hour difference. In Figure 4.3, the process described above, so one example of  $M(t)$ , the thresholded subset  $M(t)_\mu$ , the distance transform  $D(t)$  and the corresponding persistence diagram can be seen. Subsequently, the maximum persistence was computed for every six-hour-difference and was plotted over time, which can be seen in Figure 4.4. The maximum persistence for a given persistence diagram  $D$  is a common measure, because it measures the longest lifetime of a space  $P(a_i, b_i)$  in the diagram and it is especially useful when investigating a single circular structure like a hurricane. Because the circular structure should be most prevalent over time, there is probably a correlation with the maximum persistence [5]. The plot shows an oscillatory pattern, detecting the change in the diurnal cycle throughout the day.

#### 4. TOPOLOGICAL ANALYSIS OF TROPICAL CYCLONES

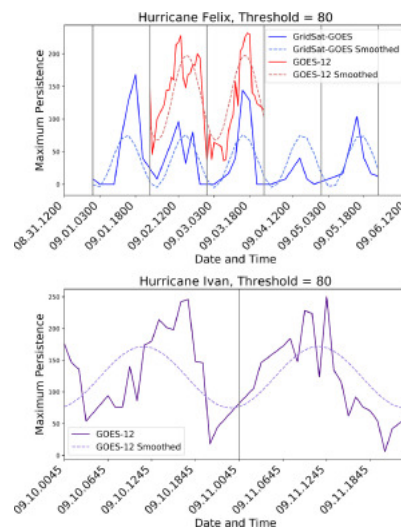


**Figure 4.4:** Maximum persistence plotted over time for all data sets using  $\mu = 80$  in addition to the reconstructed sinuoids using the inverse DFT

In order to analyze the periodicity of this pattern and to calculate the most prominent frequency in the data, the discrete Fourier transform (DFT)  $F_n$  was computed. The frequency of the most prominent signal is given by the highest peak of the power spectrum  $|F_n|^2$ , which can be used to calculate the period of the oscillatory pattern. The power spectrum of the data sets is shown in figure 4.5. Using the inverse discrete Fourier transform, the corresponding sinusoid can be reconstructed and plotted over the original data to verify that the detected signal matches the oscillatory pattern of the maximum persistence.

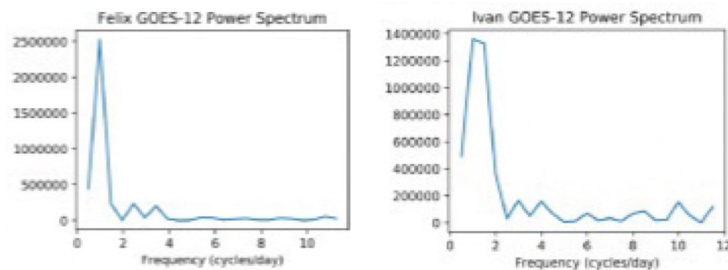


**Figure 4.5:** Power spectrum for each data set

Finally, a frequency of 0.979 cycles per day for the data set of hurricane Felix and 1.0 cycles per day for the data set of hurricane Ivan was found, which gives that the cycle is repeating every 24.5 h for the Felix data set and every 24.0 h for the Ivan data set.

## 4.2. Analysis of Tropical Cyclones using Persistent Homology

---

Thus, the approximately 24-h-patterns in the plots were also detected mathematically. In conclusion, the method presented in the paper provides a 'mathematically advanced method for automatic detection and measurement' and show one of the many applications of persistent homology.





## Chapter 5

---

# Acknowledgement

---

I thank Dr. Sara Kalisnik Hintz for introducing me to applied algebraic topology and supervising me for the duration of this thesis. She patiently answered all my questions and I am very thankful for the time she spent on me. In the end, she even became a hurricane expert.



---

## Bibliography

---

- [1] Gunnar E. Carlsson. Topological pattern recognition for point cloud data. *Acta Numerica*, 23:289 – 368, 2014.
- [2] Jason P. Dunion, Christopher D. Thorncroft, and Christopher S. Velden. The tropical cyclone diurnal cycle of mature hurricanes. *Monthly Weather Review*, 142:3900–3920, 2014.
- [3] Tomasz Kaczynski, Konstantin Mischaikow, and Marian Mrozek. *Computational Homology*. Springer-Verlag, 2004.
- [4] E. L. Navarro and G.J. Hakim. Idealized numerical modeling of the diurnal cycle of tropical cyclones. *J. Atmos. Sci.*, 73(10):4189–4201, 2016.
- [5] Sarah Tymochko, Elisabeth Munch, Jason Dunion, Kristen Corbosiero, and Ryan Torn. Using persistent homology to quantify a diurnal cycle in hurricanes. *Pattern Recognition Letters*, 133:137–143, 2020.
- [6] Wikipedia contributors. Diskrete fourier-transformation — Wikipedia, the free encyclopedia, 2023. [Online; accessed 22.06.2023].
- [7] Michio Yanai. Formation of tropical cyclones. *Reviews of Geophysics*, 2(2):367–414, 1964.



## Declaration of originality

The signed declaration of originality is a component of every semester paper, Bachelor's thesis, Master's thesis and any other degree paper undertaken during the course of studies, including the respective electronic versions.

Lecturers may also require a declaration of originality for other written papers compiled for their courses.

---

I hereby confirm that I am the sole author of the written work here enclosed and that I have compiled it in my own words. Parts excepted are corrections of form and content by the supervisor.

**Title of work** (in block letters):

**Authored by** (in block letters):

*For papers written by groups the names of all authors are required.*

**Name(s):**

**First name(s):**

.....	.....
.....	.....
.....	.....
.....	.....

With my signature I confirm that

- I have committed none of the forms of plagiarism described in the '[Citation etiquette](#)' information sheet.
- I have documented all methods, data and processes truthfully.
- I have not manipulated any data.
- I have mentioned all persons who were significant facilitators of the work.

I am aware that the work may be screened electronically for plagiarism.

**Place, date**

**Signature(s)**

.....	.....
.....	.....
.....	.....
.....	.....

*For papers written by groups the names of all authors are required. Their signatures collectively guarantee the entire content of the written paper.*